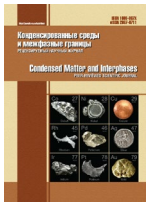

ISSN 1606-867X (Print)
ISSN 2687-0711 (Online)
Condensed Matter and Interphases
Kondensirovannye Sredy i Mezhfaznye Granitsy
https://journals.vsu.ru/kcmf/

Review

Review article
https://doi.org/10.17308/kcmf.2022.24/9256

The decisive role of biological factors in the corrosion of the D16T alloy. Review

D. V. Belov✉, S. N. Belyaev

Federal Research Centre Institute of Applied Physics of the Russian Academy of Sciences,
46 Ulyanova str., Nizhny Novgorod 603950, Russian Federation

Abstract

The biocorrosion of duralumin grade D16T has been studied and a mechanism has been proposed according to which the initiators of initial corrosion damage are reactive oxygen species (ROS) produced by micromycetes. An assumption was made about the participation of hydrogen peroxide in the mycological corrosion of the D16T alloy, which is formed both during the life of micromycetes and during the activation of oxygen by zero-valent aluminium (ZVAl). The mechanisms of intergranular, pitting and pitting corrosion of duralumin under the influence of microscopic fungi are proposed. Purpose: determination of the main biological factor initiating biocorrosion of the D16T alloy; assessment of the biological impact of the association of microscopic fungi on the alloy in order to develop scientifically grounded and effective methods of protecting aluminium and its alloys from biocorrosion by micromycetes.

The object of the study was an aluminium alloy D16T in accordance with state standard (GOST) 4784–2019 after hardening and natural ageing, which is widely used for the manufacture of load-bearing elements of structures and equipment of fuel systems of aircraft, car bodies, parts of various machines and assemblies operating at low temperatures, and in the food and pharmaceutical industries. The stages of initiation and development of biocorrosion of the D16T alloy under the influence of a consortium of moulds have been studied using a scanning electron microscope. The phase composition of the D16T corrosion products has been studied.

In the process of vital activity of microscopic fungi, reactive oxygen species are formed, initiating the biocorrosion of the D16T alloy. The initial stage of biocorrosion is caused by hydrolysis of the protective passive aluminium film. At the stage of intense biocorrosion, oxygen-containing aluminium compounds are formed in the form of a water-saturated gel. Further, as this corrosion product accumulates, its water permeability decreases. The gel undergoes "ageing" and turns into crystalline products. Conidia and hyphae of microscopic fungi adhere, are mechanically fixed on the metal surface and penetrate into the surface layers and deep into the metal, causing its corrosive destruction in the form of pitting, ulcers, and cavities. It is possible that the initiation of metal biocorrosion is a consequence of the hyperproduction of reactive oxygen species by the cells of micromycetes as a result of oxidative stress. This may be their defensive strategy aimed at destroying xenobiotic material.

The development of intergranular and pitting corrosion of the D16T alloy under the action of micromycetes occurs at the sites of contact with the exudate, which, due to a cascade of reactions with the participation of ROS, is locally enriched in hydroxide ions. The origin and development of pitting on the duralumin surface occurs in defects of the passive oxide film due to the displacement of oxygen-containing surface aluminium compounds and their interaction with corrosive OH– and ROS anions. Hydrogen peroxide, as an intermediate product of the metabolism of micromycetes, on the surface of the D16T alloy can participate in the Fenton process or decompose heterogeneously, also provoking the development of aluminium biocorrosion.

Keywords: Biocorrosion, Mycological corrosion, Duralumin, D16T, Zero-valent aluminium, ZVAl, Micromycetes, Microscopic fungi, Reactive oxygen species, ROS, Superoxide anion radical, Hydrogen peroxide, Intergranular corrosion, Pitting corrosion

Acknowledgements: The authors express their gratitude to G. A. Gevorgyan and M. V. Maksimov for help in performing macro- and microstructural analysis and studies on an electron microscope (JSC Central Research Institute Burevestnik, Nizhny Novgorod 603950, Sormovskoe shosse, 1a).

✉ Denis. V. Belov, belov.denbel2013@yandex.ru

For citation: Belov D. V., Belyaev S. N. The decisive role of biological factors in the corrosion of the D16T alloy. Review. *Condensed Matter and Interphases*. 2022;24(2): 155–181. https://doi.org/10.17308/kcmf.2022.24/9256

Для цитирования: Белов Д. В., Беляев С. Н. Об определяющей роли биологических факторов в коррозии сплава Д16Т. Обзор. Конденсированные среды и межфазные границы. *Конденсированные среды и межфазные границы*. 2022;24(2): 155–181. https://doi.org/10.17308/kcmf.2022.24/9256

1. Introduction

The most active biological agents ubiquitous in soil, water, and air are mould or microscopic fungi (micromycetes). Often they prevail over other microorganisms and have the greatest potential for impact on almost all infrastructure and human industrial and household activities. Micromycetes are active agents initiating microbiological corrosion of most metals and alloys. The species diversity of microscopic fungi, their high adaptability to living conditions, and powerful enzymatic apparatus lead to significant amounts of damage to metal materials by them. The microbiological corrosion (biocorrosion) of metals is the destruction caused by the direct or indirect action of microorganisms. The biocorrosion of metals by micromycetes in atmospheric and soil conditions, for example, in well-ventilated places with favourable temperature and humidity characteristics, with the presence of contaminants on the metal surface is especially characteristic [1].

The microbial corrosion of metals is a serious environmental and economic problem. In most cases, the corrosion of metals occurs in an oxygen-containing environment. Among the microorganisms involved in the corrosion of metals, the most active ones are aerobic. However, among anaerobic microorganisms, there are those that are capable of initiating and accelerating the oxidation of metals. Some of these microbes can consume molecular hydrogen, abiotically formed during the oxidation of metals. Due to the occurrence of coupled reactions, the anaerobic oxidation of metals becomes thermodynamically favourable. Additionally, extracellular enzymes, such as hydrogenases, accelerate the oxidation of metals. Organic electron carriers such as flavins, phenazines, humic substances can replace molecular hydrogen as an electron carrier between metal and living cells. Direct electron transfer without intermediaries from oxidising metal to microbial cells is also possible [2–5].

The role of biofilms in the corrosion of metals. First discovered in 1978, the existence of a specific form of bacteria in the form of biofilms [6] was recognised as the predominant form of microbial life on our planet. Biofilms are defined as a special form of organisation of microorganisms formed at the interface between two phases, intensively exchanging genetic information and capable of coordinating their behaviour through the secretion of molecular signals – *Quorum Sensing*. The study of biofilms has many practical applications, for example, in medicine, in the ecology of natural and industrial waters, and in hydrometallurgy. The practical significance of the study of planktonic and biofilm forms of habitation of corrosive microorganisms in aquatic environments is due to the relevance of increasing the efficiency of biocidal protection of buildings and structures.

The issue of the decisive role of bacterial biofilms in the corrosion of metals is widely discussed in the literature [7–12]. However, the issue of the effect of biofilms of microscopic fungi has been little studied. In our opinion, biofilms of micromycetes are one of the determining factors in the corrosion processes of metals.

A bacterial biofilm is a collection of surface-associated microbial cells enclosed in a matrix of an extracellular polymeric substance, predominantly a polysaccharide material. In [13], the decisive role of the adhesion of bacteria *Pseudomonas fluorescens* and *Desulfovibrio desulfuricans* to metal surfaces in their corrosion was reported. The authors provided evidence that the substance involved in the primary adhesion of bacteria to the surface of mild steel is of a polysaccharide nature. This substance is present in the outer membrane of bacterial cells in the form of lipopolysaccharide [14].

Mycelial fungi can organise multicellular, highly structured consortia known as fungal biofilms that form stable communities on a variety of biotic and abiotic surfaces. Most of the research is focused on the study of planktonic

forms of micromycetes. The analysis of the literature data showed that filamentous fungi are ubiquitous in various aquatic environments, including drinking water distribution systems. Within such closed water supply systems, consortiums of microscopic fungi, which form biofilms, develop. According to [15], the biofilm isolated from the drinking water distribution system included the following micromycetes: *Aspergillus* sp., *Alternaria* sp., *Botrytis* sp., *Cladosporium* sp., *Penicillium* sp.

The typical morphology of a biofilm of microscopic fungi is described as a complex three-dimensional structure of heterogeneous surface-associated colonies consisting of filamentous hyphae (chains of elongated cells), pseudohyphal cells, yeast-like cells, and various forms of extracellular matrix (Fig. 1) [16]. For example, micromycete *Aspergillus fumigatus* produces *in vitro* an extracellular hydrophobic matrix with typical characteristics of a biofilm, consisting of galactomannan, α-1,3-glucans, monosaccharides, polyols, melanin, and proteins (antigens and hydrophobins) [17, 18].

During the initial stages of biofilm growth and development, the formation of a layer of substances surrounding the fungus is observed. This layer is involved in the binding of cells to each other (cohesion) and in their interaction with the surface of the substrate (adhesion). These substances provide the structural basis of the forming microfilm. Each microscopic fungus has its own pattern of biofilm development.

Microorganisms have now been shown to be able to adhere to virtually any surface. Surface-associated micromycetes, which form biofilms, have a special phenotype that differs from planktonic organisms. They have specific mechanisms of attachment to the surface, which are regulated by various characteristics of the nutrient medium, substrate, and cell surface [19].

In nature, adhesion is a widespread phenomenon inherent in many microorganisms, which allows them to colonise their habitats. The

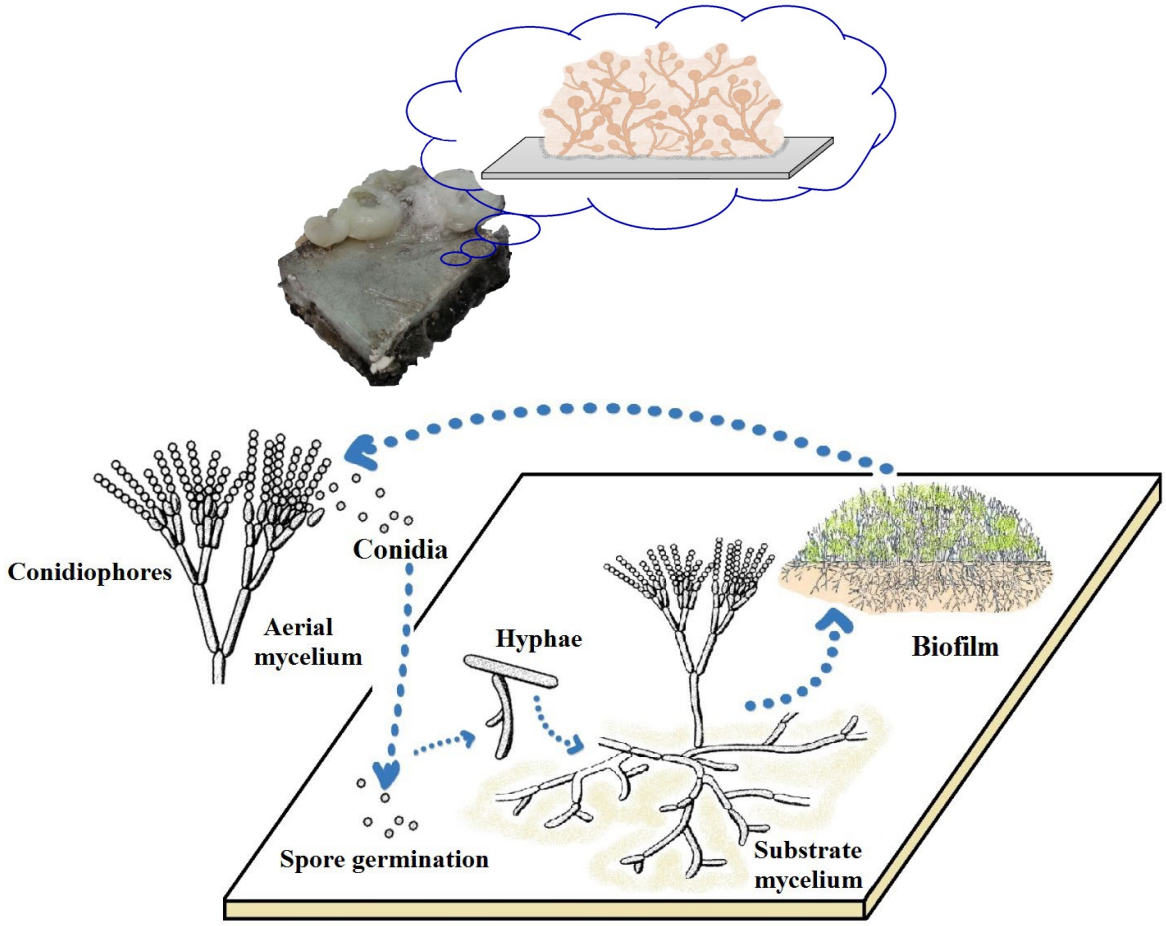

Fig. 1. Scheme of the formation of a biofilm of micromycetes on the surface of a metal

adhesive ability of micromycetes determines their further colonisation of the metal surface. The stage of attack of micromycetes on the metal surface following the primary adsorption is characterised by the invasive (from lat. *invasio* – invasion, attack) growth of a microorganism. Proteolytic, lipolytic enzymes of fungi (proteases, hyaluronidase, phospholipase, lipase, etc.) are involved in the destruction of the surface structural elements of the protective film on the metal surface and enable its further colonisation and penetration (from lat. *penetratio* – penetrate). The pathogenicity factors of microscopic fungi include adhesins. Adhesins are areas of the fungi surface (proteins, carbohydrate parts of cell wall mannoproteins, etc.) that ensure the attachment of a microorganism to a solid substrate. Adhesins of micromycetes differ by specificity and allow them to adhere to different solid substrates. [20]. The study [21] reports that the adhesion of microorganisms is the initial stage of the biofouling of materials, including metals, in air and water environments. The authors studied the adhesion of the conidia of a microscopic fungus, *Trichoderma viride*, to the surface of metals differing in oxidising potentials, and determined the quantitative kinetic parameters characterising the stage of adhesion of the conidia of micromycetes.

Now, scanning electron microscopy is widely used to visualise micromycete biofilms [22]. In the study [23], the stages of biofilm formation of the *Aspergillus fumigatus* micromycete were studied using confocal laser scanning microscopy. The authors of the study [24] carried out a structural analysis of the biofilms of the *Aspergillus niger* micromycete using the same method.

In our studies, we observed the biofilm formation of microscopic fungi on all surfaces of corroding metals. Biofilms of microscopic fungi on the surface of the D16T alloy are shown in Figs. 2 and 3.

Recent advances in molecular techniques and confocal microscopy have shown that biofilm formation is a natural and preferred form of fungal growth and a major cause of persistent infections in humans. The study [25] presents microscopic, spectroscopic, and microsensor methods for studying biofilms. Analytical methods for studying extracellular polymeric substances, in particular, polysaccharides and proteins, are generalised.

The presence of microorganisms on the surface of a material can significantly affect its performance. Surface-mediated microbial growth and the formation of a biofilm on a solid substrate provokes its further biofouling. The presence of biofilms can promote interfacial physicochemical reactions, which are undesirable under abiotic conditions. Therefore, the generally accepted concept of biocorrosion is expanding. The existing definition of biocorrosion can be extended by noting that these are changes in

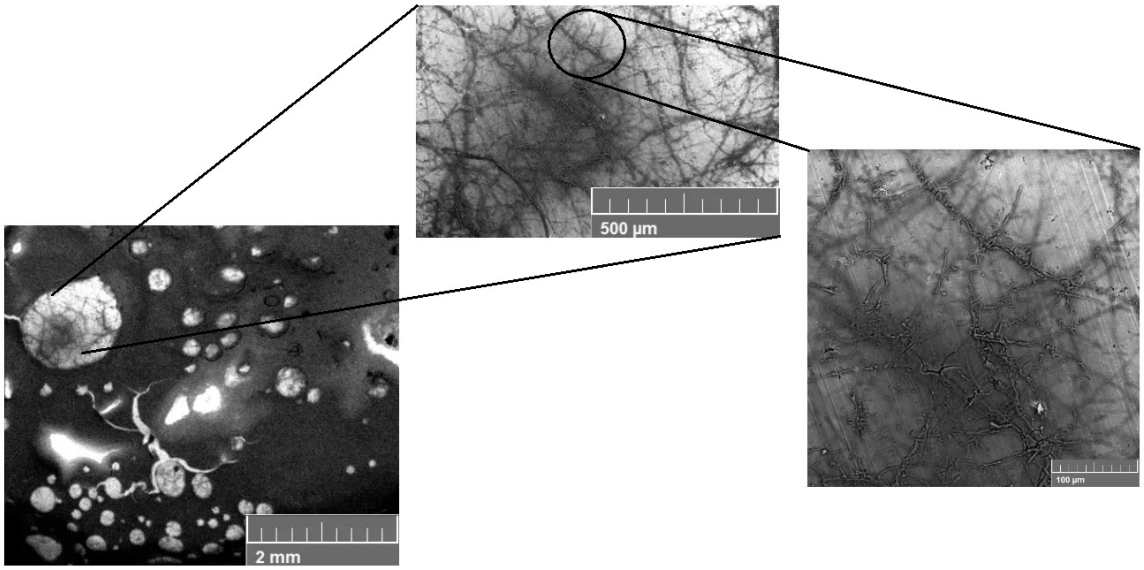

Fig. 2. Formation of a biofilm of a consortium of microscopic fungi on the surface of the D16T alloy

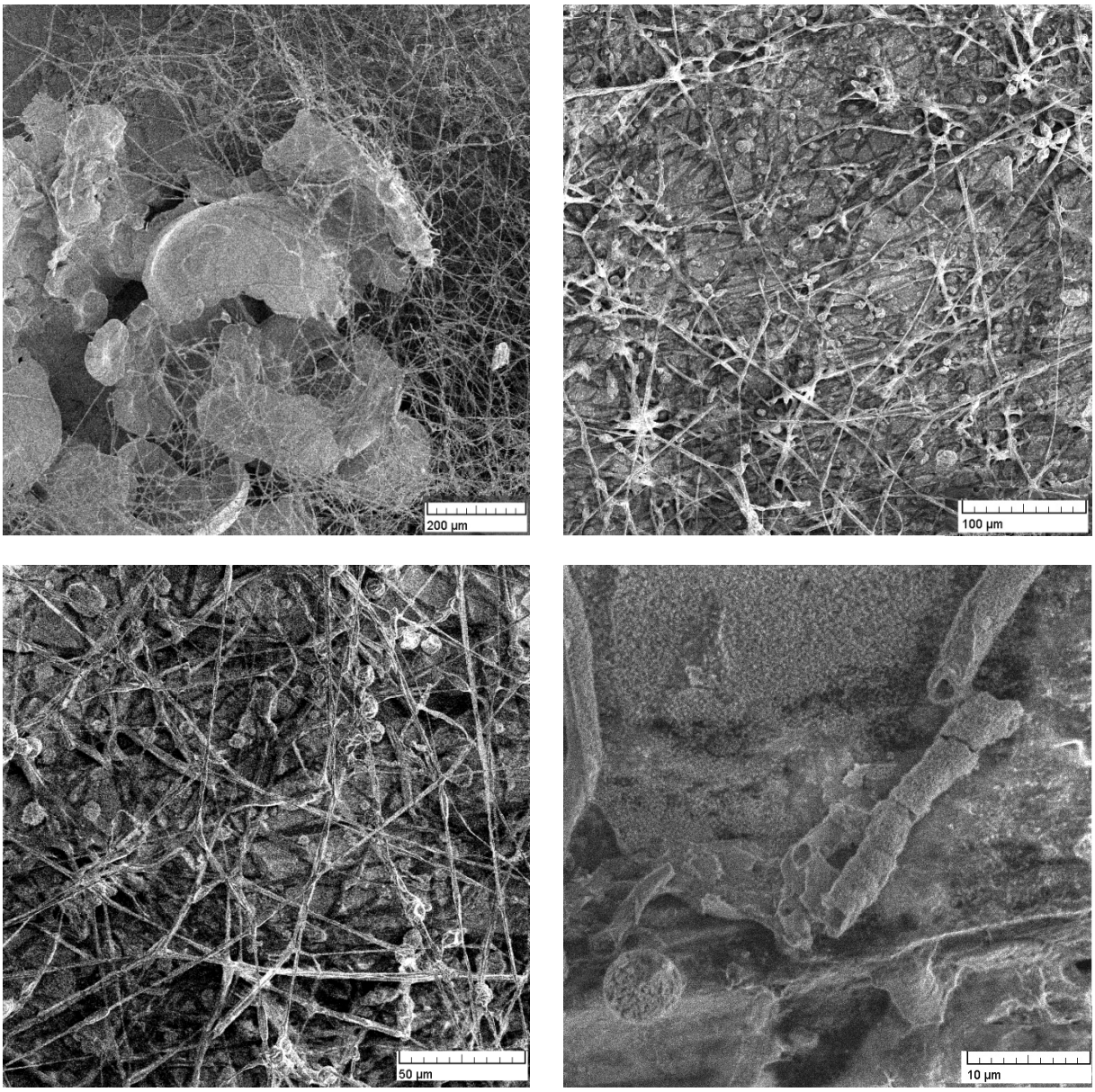

Fig. 3. Photographs of a biofilm of a consortium of microscopic fungi on the surface of the D16T alloy

the properties of metallic materials caused by the formation of a biofilm or biofouling layer. The biocorrosion of metals can be considered a consequence of coupled biological and abiotic reactions of electron transfer from metals to microbial cells [26].

The detailed mechanisms of biocorrosion are still poorly understood. Thus, in the article [27], the main attention of researchers was focused on studying the effect of biomineralisation processes occurring on metal surfaces, on the biocorrosion of metals, and the effect of extracellular enzymes active in the biofilm matrix on electrochemical reactions at the biofilm–metal interface.

It is generally accepted that the biocorrosion of metals under the influence of microscopic fungi is indirect and occurs when exposed to aggressive media formed as a result of their vital activity. However, we have shown in experiments that micromycetes are directly involved in the destruction of the surface of metals.

The role of reactive oxygen species (ROS) in the biocorrosion of metals. The production of ROS, including the superoxide anion radical ($O_2^{\bullet -}$), hydrogen peroxide (H_2O_2) and hydroxyl radicals ($HO^{\bullet}$), is a characteristic phenomenon of all living organisms, including mould fungi. ROS play various roles in cellular defence and

in the transmission of signals that control the differentiation, development, and pathogenesis of micromycete cells [28]. ROS regulate the germination, development, and intercellular interactions in microscopic fungi. The study [29] points out that ROS are formed in microscopic fungi over the course of metabolic activity. The formation of ROS increases under the influence of various stress factors, including starvation, light, mechanical damage, and interaction with other living objects. The regulation of ROS content is the most important aspect in the development of a fungal organism. The review considers the sources of ROS in fungal cells, sensors, and pathways of ROS signal transduction. A detailed description of antioxidant protection in different classes of microscopic fungi is provided.

Active oxygen metabolites - hydrogen peroxide H_2O_2 and the superoxide anion radical $O_2^{\bullet-}$ are always present in cells in low concentrations, participating, among other things, in intra- and intercellular signalling [30]. Hydrogen peroxide is considered to be a marker of oxidative stress [31]. Hydrogen peroxide is a by-product in various cellular processes and the end product of many metabolic reactions.

In the physiological range of concentrations (from 1 nM to 0.1–0.5 μM), H_2O_2 acts as a signalling molecule, takes part in the processes of cell differentiation, migration, and proliferation [32, 33]. With an increase in concentration to 1–10 μM, H_2O_2 causes the arrest of the cell cycle, which is usually restored and even accelerated in the case of a successful adaptation to oxidative stress. At high concentrations (⩾10 μM H_2O_2) oxidative stress prevails, adaptation does not occur, and apoptosis starts. The boundaries of these reactions are relative and strongly depend on the cell type, cultivation conditions, and heterogeneous distribution of H_2O_2 in the cell, which makes the concept of the average intracellular concentration of H_2O_2 unacceptable [34].

The ability of soil micromycetes to synthesise and release hydrogen peroxide into the environment is widely known [35]. The study [36] reports on the ability of a microscopic fungus, *Trichoderma guizhouense,* to synthesise and accumulate significant amounts of hydrogen peroxide. The formation of H_2O_2 by fungi can occur through two main metabolic reactions: as a by-product of oxidation by FAD-dependent oxidases such as glucose oxidase or amino acid oxidases [37–40], and by dismutation of the superoxide anion radical $O_2^{\bullet-}$ by superoxide dismutases (SOD) [41].

In [42], it was reported that the key role in the development of the phytopathogenic fungus *Fusarium graminearum* depends on the balanced dynamics of the formation of reactive oxygen species, in particular hydrogen peroxide. In [43], 50 strains of fungi belonging to different types of basidiomycetes were tested for the ability to synthesise and release H_2O_2. A comparative evaluation on the ability of microorganisms to decolorise synthetic dyes was carried out. Hydrogen peroxide is involved in the decomposition of lignin and cellulose by white and brown rot fungi as a co-substrate [44, 45]. In addition, it was shown that H_2O_2 plays a key role in the degradation of lignocellulose [46].

The study [47] proved the ability of mycelial fungus *Stilbella aciculosa* to produce an extracellular superoxide anion radical during cell differentiation. In [48–50], detailed descriptions of the chemical and biochemical properties of $O_2^{\bullet-}$ were presented.

Superoxide anion radicals during initiation of biocorrosion of metals. In our own previous studies [51, 52] it was shown that $O_2^{\bullet-}$, formed during the life of microscopic fungi, can pass into the pericellular environment and act as an initiator of physicochemical processes leading to deep destruction of metals. It is known that $O_2^{\bullet-}$ in an aqueous solution exists in the form of an equilibrium mixture of a base and a conjugated acid - a hydroperoxide radical. At pH>7, the equilibrium is shifted towards $O_2^{\bullet-}$, the radicals of an equilibrium mixture in aqueous solutions rapidly transform into stable products as a result of parallel reactions [53, 54] in accordance with reaction schemes (1)–(4):

$$HO_2^{\bullet} \leftrightarrow O_2^{\bullet-} + H^+, K_a = 1.6\times10^{-5}, \quad pK_a = 4.60\pm0.15, \quad (1)$$

$$HO_2^{\bullet} + HO_2^{\bullet} \rightarrow O_2 + H_2O_2, \quad k = (8.60\pm0.62)\times10^5\ M^{-1}s^{-1}, \quad (2)$$

$$O_2^{\bullet-} + O_2^{\bullet-} + 2\ H_2O \rightarrow O_2 + H_2O_2 + 2\ OH^-, \quad k<0.35\ M^{-1}s^{-1}, \quad (3)$$

$HO_2^{\bullet} + O_2^{\bullet -} + H_2O \rightarrow O_2 + H_2O_2 + OH^-$,
$k = (1.02 \pm 0.49) \times 10^8\ M^{-1}s^{-1}$. (4)

As a result of the cascade of these reactions, corrosive agents accumulate in the medium, initiating metal corrosion.

The participation of hydrogen peroxide in the corrosion of metals. In a number of literary sources, the issue of the effect of hydrogen peroxide on metal corrosion and its participation in the initiation and stimulation of metal corrosion is considered [55, 56].

For example, the authors of [57, 58] studied the effect of hydrogen peroxide on the corrosion of stainless steel. The study presents the characteristics of oxide films formed on stainless steel when exposed to H_2O_2 and O_2 in water. In [59], the corrosion of various stainless steels in chloride-containing alkaline solutions of hydrogen peroxide was studied by electrochemical methods. The authors concluded that alkaline solutions of hydrogen peroxide cause the corrosion of stainless steels to varying degrees, regardless of the content of chloride ions, and their corrosion activity increases with an increasing content of H_2O_2.

Titanium, currently widely used in dental implantology and orthopaedics due to its excellent corrosion resistance and mechanical properties, has proven to be unstable in environments containing H_2O_2 [60–62]. The corrosion of titanium in a hydrogen peroxide solution in an alkaline medium was investigated in [63]. The authors proposed a reaction mechanism based on the interaction of titanium oxide with perhydroxyl ion (HO_2^-).

The mechanism of aluminium dissolution in alkaline media. From a thermodynamic point of view, aluminium is an active metal, which is determined by the negative value of its equilibrium electrode potentials (–1.662 V, $Al - 3\bar{e} = Al^{3+}$; –2.35 V, $Al + 4OH^- - 3\bar{e} = [Al(OH)_4]^-$) [64].

The high corrosion resistance of aluminium under natural conditions is due to the presence of a multilayer passive film on its surface. In air, pure aluminium is covered with a strong oxide film 5–10 nm thick, which protects it from further oxidation [65]. It is formed as a result of oxidation of the surface layer of a pure metal by air and water oxygen molecules and reaches a thickness that ensures it is impervious to gases. To date, a lot of information about its structure has been accumulated. According to some data [66], under natural conditions at a temperature of 20 – 90 °C it consists of three layers: an amorphous oxide or hydroxide several nm thick located directly on the aluminium surface; a layer of pseudo-boehmite $Al_2O_3 \cdot 1.3H_2O$ located in between; and a layer of bayerite $Al_2O_3 \cdot 3H_2O$, a few microns thick on the top of it. According to other data [67–69], the protective film is a thin barrier layer of monohydrate orthorhombic boehmite γ-AlO(OH) adjacent to the metal surface and a thicker outer layer of crystalline oxide consisting of bayerite or hydrargillite $Al_2O_3 \cdot 3H_2O$. Some authors noted that under normal conditions, a protective X-ray amorphous oxide layer with a thickness of 4–10 nm was formed on the surface of the aluminium, which may include bayerite $Al(OH)_3$ and boehmite AlO(OH) [70–72]. The determining influence on the biocorrosion of the D16T alloy is exerted by the composition and state of the passivating layer on its surface [73–76].

Metallic aluminium actively reacts with various oxidising agents, including O_2 and H_2O. For example, the reaction products of aluminium with water are hydrogen and solid oxidation products formed according to schemes (5)–(7):

$2Al + 3H_2O = Al_2O_3 + 3H_2$, (5)
$2Al + 4H_2O = 2AlO(OH) + 3H_2$, (6)
$2Al + 6H_2O = 2Al(OH)_3 + 3H_2$. (7)

The mechanism of aluminium oxidation has been studied in detail by a number of authors in [77 – 80]. The electrochemical dissolution of aluminium, according to the authors of [81, 82], includes at least two conjugated processes: the formation of a protective passive oxide film ($Al + 3OH^- - 3e = AlO(OH) + H_2O$) and its chemical dissolution with the formation of soluble aluminates. The authors of [83] believe that in solutions with pH < 12, the rate of formation of a passive film is higher than the rate of its dissolution. Therefore, the rate of aluminium corrosion is controlled by the stage of removing hydroxide films from the metal surface, the dissolution of which is determined by the diffusion of $[Al(OH)_4]^-$ and OH^-. It was pointed out in [84] that the corrosion of pure aluminium

in an alkaline solution can be explained by the operation of a short-circuited corrosion cell and includes the stages of formation and dissolution of a natural oxide film with simultaneous reduction of water molecules.

The development of modern methods for a reliable assessment of the biodamage of materials, the prediction of the effect of biocorrosion on the mechanical characteristics of products and the safety of their further operation are important and urgent tasks. Therefore, the study of the problem of microbiological corrosion of metals is of great importance for the development of ways to increase the durability of metal materials and products and structures based on them. Aluminium and its alloys are used as the main structural material for the manufacture of equipment for the food industry, aircraft, and spacecraft [85].

Now, the mechanism of metal biocorrosion under the influence of microscopic fungi has not been fully studied, and the existing methods of protection against it are ineffective [86, 87]. The biocorrosion of aluminium and alloys based on it is still a poorly studied issue and causes a lot of controversy in the scientific world.

Purpose: determination of the main biological factor initiating biocorrosion of the D16T alloy; assessment of the biological impact of the association of microscopic fungi on the alloy in order to develop scientifically grounded and effective methods of protecting aluminium and its alloys from biocorrosion by micromycetes.

The focus of the study was the aluminium alloy D16T in accordance with state standard (GOST) 4784-2019 after hardening and natural ageing, which is widely used for the manufacture of load-bearing elements of structures and equipment of fuel systems of aircraft, car bodies, parts of various machines and assembles operating at low temperatures, in the food and pharmaceutical industries. In our previous study, we investigated the biocorrosion of AD0 grade aluminium and aluminium-based alloys: B65, D16, AMg6 [88, 89].

Using a scanning electron microscope, the stages of initiation and development of biocorrosion of the D16T alloy under the influence of a consortium of mould fungi were studied. The phase composition of D16T corrosion products has been studied.

2. Experimental

In the experiments, a consortium of natural strains of microscopic fungi was used, the spores of which were isolated from the air of industrial premises and from washings from the working surfaces of equipment. The surface of Czapek–Dox solid nutrient medium with sucrose, poured into Petri dishes, was inoculated with micromycete spores. Petri dishes with a dense nutrient medium were open in the working areas of production facilities for several hours, after they were placed in a thermostat for the development of lawn of micromycetes. According to the second method, swabbings of equipment surfaces were applied to the surface of a dense nutrient medium in the form of a suspension of micromycete spores in physiological solution (0.9% NaCl), obtained by wiping the surfaces with a cotton swab. Next, the prepared metal samples were placed on the lawns of micromycete consortiums. The experiment lasted at least 10 months at a temperature of (27±2) °C in a biological thermostat. A comparison was performed with control samples placed on sterile nutrient media. The experimental technique is described in detail in [51, 52, 90].

The identification of micromycetes from the surface of metal samples was carried out based on their morphological and cultural features, using an identification guide [91, 92].

The results of the research showed that the mycobiota of aluminium alloys was mainly represented by the following genera of micromycetes: *Alternata*, *Aspergillus Mucor* and *Penicillium*.

Preparation of samples and the assessment of biocorrosive damage. Metal samples in the form of 30x20x15 mm and 20×20×15 mm bars were ground to obtain a smooth surface and polished to a mirror finish. Then they were washed with water, the surface was degreased with carbon tetrachloride, ethyl alcohol, and dried.

Corrosion products after exposure were removed mechanically with a brush with polymer bristles. Corrosion products strongly adhering to the surface was removed by ultrasonic cleaning with an ultrasonic frequency of 20–30 kHz. The

medium was distilled water with a temperature of (20±2) °C. For the identification of the most severe biodamage, the samples were analysed visually. To reveal the microstructure of the surface, the samples were etched in a Keller solution of the following composition: HF (48 %) 1.0 ml; HCl (ρ = 1.19 g/cm^3) 1.5 ml; HNO_3 (ρ = 1.42 g/cm^3) 2.5 ml; H_2O 95.0 ml.

The macroscopic study of the surface of the samples was carried out using an MBS-2 light microscope. Microstructural studies in the cross section of corroded samples were carried using an optical microscope MT 753F. The fine structure of the corroded samples was analysed using TESCAN VEGA 3 XMH scanning electron microscope with a lanthanum hexaboride LaB_6 cathode. Qualitative and semi-quantitative analysis of chemical elements present in the composition of corrosion products after exposing the samples to the lawns of micromycete consortiums was carried out using energy dispersive X-ray spectroscopy (EDS-analysis). The equipment for EDS analysis was an energy-dispersive spectrometer based on a semiconductor silicon-drift detector with nitrogen-free cooling, mounted on a scanning electron microscope column with a range of detected elements from Be(4) to Pu(94).

X-ray phase analysis of sample biocorrosion products was carried out by the standard method using a Dron-3M diffractometer with monochromatised CuK_a-radiation in a Bragg-Brentano geometry. The identification of crystalline phases was carried out by comparison of the obtained experimental values of interplanar distances and relative intensities with the reference ones.

Identification of ROS. For the registration of the extracellular superoxide anion radical $O_2^{\bullet-}$ nitro blue tetrazolium chloride dye (NBT^{2+}) $2Cl^-$ was used. This dye is widely used for these purposes in various chemical and biochemical studies [93, 94], it is reduced to mono- and diformazans characterised by absorption maxima at 525 nm (ε_{525} = 23400 $M^{-1}cm^{-1}$ in ethanol) and 605 nm (ε_{605} = 40200 $M^{-1}cm^{-1}$ in a mixture of ethanol – chloroform), respectively [95]. Formazan was eluted from the aqueous extract using a dimethyl sulfoxide – chloroform mixture in a 2:1 volume ratio. The concentration of coloured formazan in the analysed samples was determined using a UV-3600i Plus spectrophotometer (Shimadzu, Japan). As a control, a dye solution with the addition of superoxide dismutase (SOD, 15 Units) was used, which at pH = 7 and a temperature of (20–25) °C with a rate constant of $k = (1.8 – 2.3)\times10^9$ $M^{-1}s^{-1}$ with absolute specificity, catalyses the reaction of dismutation of the superoxide anion radical into H_2O_2 and O_2 [96–98]. The research methodology is described in detail in [52, 90, 99].

Also, the formation of $O_2^{\bullet-}$ was confirmed by the spectrophotometric method using adrenaline [100]. For experiments, we used a pharmacopoeial preparation of epinephrine hydrochloride (1 mM, pH = 7, treatment time 15 min), which in the presence of $O_2^{\bullet-}$ turns into adrenochrome [101]. Adrenochrome formation was monitored spectrophotometrically using a UV-3600i Plus (Shimadzu, Japan) at λ_{max} = 347 nm. The reaction constant of the superoxide anion radical with adrenaline is $(4.0–5.6)\times10^4$ $M^{-1}s^{-1}$ [102, 103]. The superoxide specificity of the adrenaline-adrenochrome system was confirmed by a significant (up to 75 %) inhibition of the detection of the superoxide anion radical in the presence of superoxide dismutase (SOD, 15 Units). 200 µl of 0.1 % aqueous solution of epinephrine hydrochloride was added to 2 ml of liquid exudate freed from micromycete cells. After 15-mins of incubation, spectrophotometric measurement was performed.

For the determination of hydrogen peroxide in the liquid exudate formed during aluminium biocorrosion, the so-called FOX method was used. The FOX-method is based on the change in colour of the xylenol orange dye (λ_{max} = 540 nm, ε_{540} = 26800 $M^{-1}sm^{-1}$). The reaction reagent included: 500 µM iron ammonium sulphate; 50 mM sulphuric acid; 100 mM sorbitol; 250 µM xylenol orange [104]. The measurements were carried out using a UV-3600i Plus spectrophotometer (Shimadzu, Japan) at a wavelength of 540 nm. The amount of hydrogen peroxide was calculated using calibration curves.

The concentration of H_2O_2 was measured by the titanium method [105, 106].

3. Results and discussion

Interactions in the “metal - micromycetes” system at the stage of initiation of biocorrosion

should be considered as a set of physicochemical, chemical, and biochemical processes occurring at the interfaces between surface oxygen compounds of aluminium, forming its protective passive film, and an aqueous solution of exudate formed during the life of cells microscopic fungi, with the involvement of environmental components - oxygen and water.

The first stage mycological corrosion of metal is characterised by the development of colonies of micromycetes. For some period of time (3-5 days) they adapt, grow and develop, then exometabolites appear and locally accumulate, initiating the primary processes of destruction of the metal surface. Biocorrosion begins from the ends and on the side surfaces of the samples with the appearance of exometabolites or the so-called exudate in the form of a transparent mobile liquid. Where there is a local concentration of exometabolites, they interact with the components of the passive protective metal film. This is possible only with the participation of water, the film of which can appear on the metal surface due to capillary condensation. This will be facilitated by the mycelium of microscopic fungi fixed on the surface of the metal. Due to the energy inhomogeneity of the metal surface, its various parts will interact with living cells and electrolytes with different intensities [107]. This leads to the uneven formation of corrosion centres. Following this, electrochemical processes on the metal surface take part in the general mechanism and cathodic and anodic depolarisations occur. When the surface structures protecting the base metal are loosened, hyphae and conidia of microscopic fungi penetrate deep into the metal and interact with the components of the corrosive medium.

In these experiments, we simulated conditions close to the real operating conditions of metals and alloys, using artificially prepared nutrient media for cultivating micromycetes.

We have assessed corrosion damage during all stages of biocorrosion with a detailed analysis of the stages of the process, the appearance of samples, the area and depth of corrosion damage:

- the appearance of exudate in the form of a transparent liquid from the ends and on the side surfaces of the samples and the initiation of biocorrosion;

- fouling of the sample surface with mycelium followed by the introduction of hyphae into the loose surface structures of the metal;

- transformation of a transparent exudate into a mobile gel, easily removed from the metal surface;

- the transformation of the gel into jelly;

- ageing and crystallisation of jelly with the formation of amorphous corrosion products;

- the formation of solid crystalline corrosion products that firmly adhere to the surface of the sample.

In the case of electrochemical corrosion of aluminium, a similar sequence of processes is not observed. We will consider these stages in more detail.

The initial stage of biocorrosion is the local appearance on the surface of a micromycete consortium lawn in contact with the metal, an exudate in the form of a transparent and highly mobile liquid with a pH of 8–9 (Fig. 4). The formation of an exudate was also noticed in the study of aluminium biocorrosion under the influence of individual strains of micromycetes on it [90]. Similarities can also be traced in the

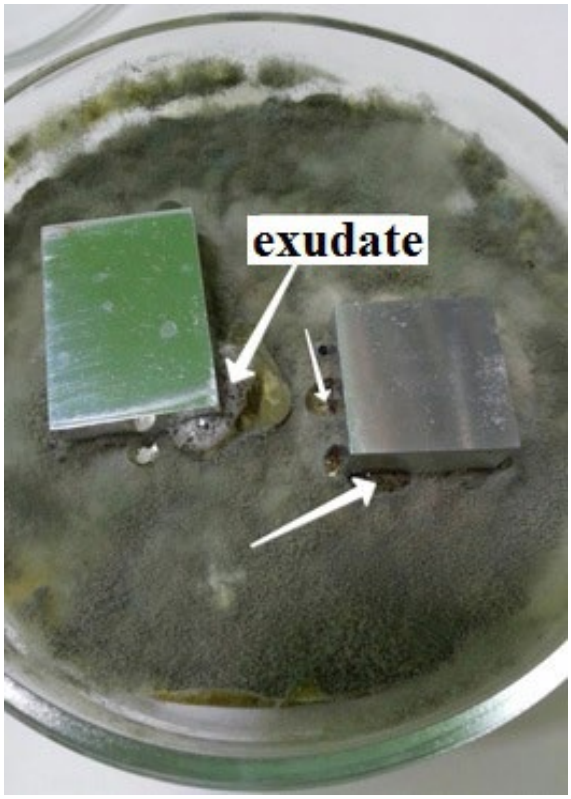

Fig. 4. Drops of exudate on the lateral surfaces of corrosive samples (shown by arrows)

staging of the process and general observations.

Within two to three days from the beginning of the experiment, the consistency of the exudate becomes gel-like (Fig. 5). A transparent gel eventually turns into a jelly, undergoes ageing and its structural changes occur: compaction, turbidity and crystallisation, and the pH value gradually shifts to neutral.

The study of the surface morphology of the samples at the initial stage of biocorrosion showed that the mycelium of micromycetes is fixed on the surface of the samples (Fig. 6) and then penetrates through the protective film deep into the metal (Fig. 7).

After adsorption and fixation of hyphae of micromycetes on certain energetically favourable areas of the alloy surface, hyphae and conidia of micromycetes are introduced into the loose and defective sites of the surface layers of the metal. In these sites, pittings and ulcers are subsequently found (Fig. 8).

Biocorrosion mechanism of the aluminium. The biocorrosion of aluminium is a complex phenomenon that includes at least three processes [89]: 1) the interaction of the components of the protective passive film and pure metal with reactive oxygen species released during the life of microscopic fungi; 2) electrochemical corrosion of the alloy due to the operation of short-circuited galvanic cells; 3) reductive activation of oxygen with the participation of zero-valent aluminium ZVAl with the formation of hydrogen peroxide, which is involved in the direct destruction of the metal and in the cascade of ROS reactions, as well as heterogeneous decomposition of hydrogen peroxide by a mechanism similar to the Fenton reaction.

Intense corrosion damage to the surface of the D16T alloy at the initial stages of exposure to microscopic fungi suggests that the corrosive

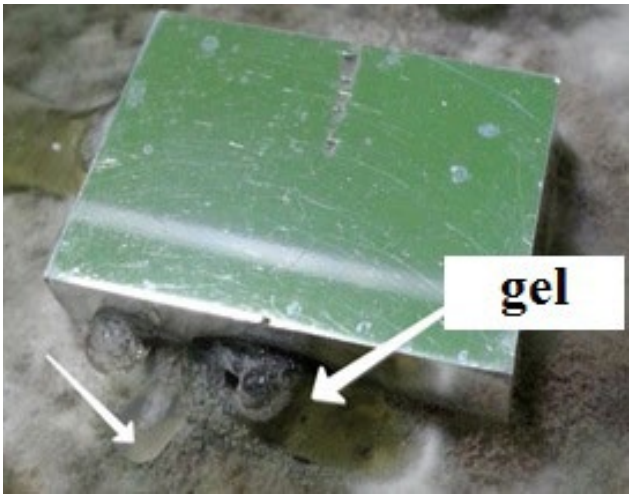

Fig. 5. Translucent gel at the sites of exudate formation (shown by arrows)

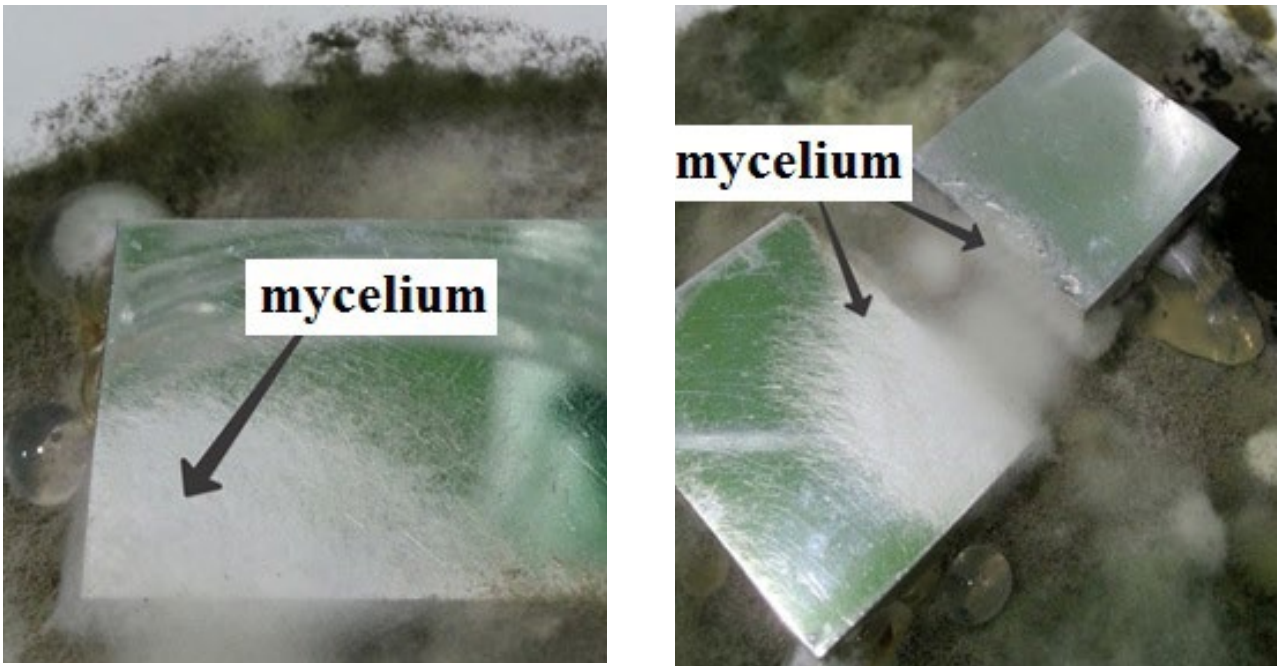

Fig. 6. Adhesion of mycelium of micromycetes on the surface of the samples and their gradual overgrowth (shown by arrows)

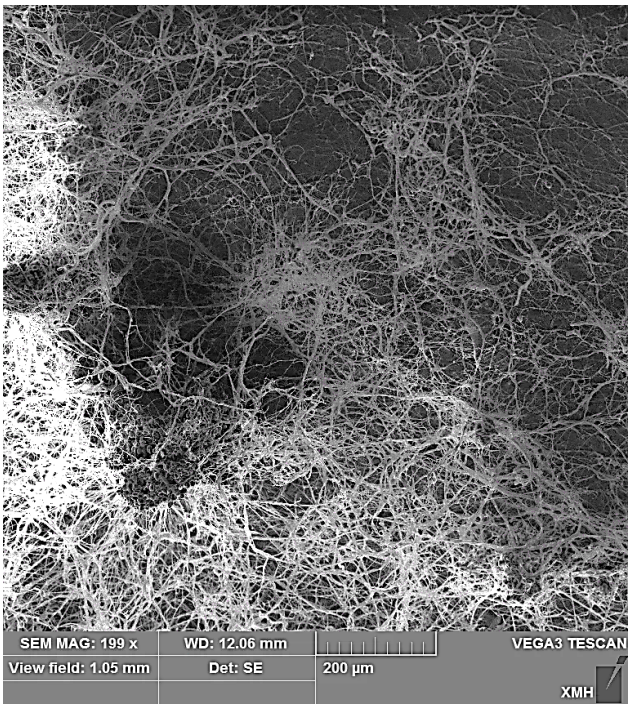

Fig. 7. Micrograph of the sample surface with mycelium filaments (hyphae) of micromycetes

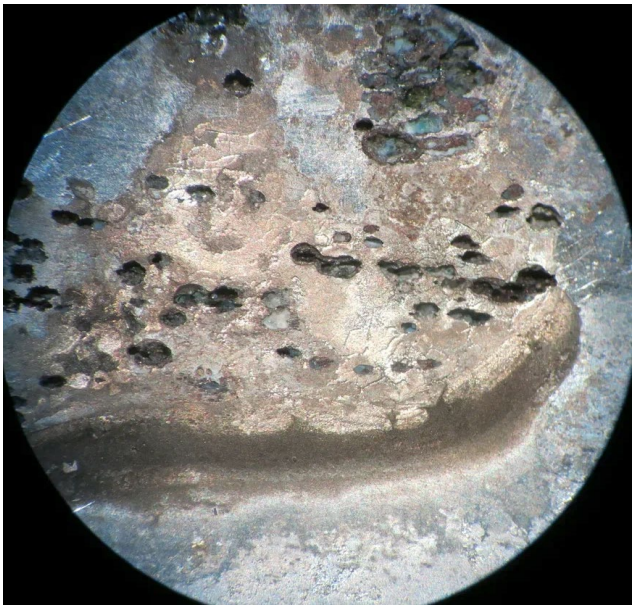

Fig. 8. Surface of the sample after exposure to a consortium of micromycetes for 60 days. Pitting is visible. Some pits merge into ulcers and cavities

agents are, first of all, OH^- and H_2O_2. The cascade of reduction reactions involving water molecules that proceed according to the electrochemical mechanism on the microcathode areas of the surface of the corroding aluminium alloy can serves as the source of OH^--ions, while oxidative dissolution of aluminium alloy occurs on the microanode areas. It is difficult to explain the continuous accumulation of OH^- ions during the initial stages of biocorrosion using only the electrochemical mechanism of corrosion. During this period, no obvious corrosion damage is observed, however, exudate drops in direct contact with the surfaces of the samples grow in volume and, at the same time, their pH value increases (up to 10–11). Upon exposure to microscopic fungi OH^- ions constantly accumulate in the liquid exudate in sites of direct contact with the metal, which is possible only as a result of the occurrence of respiratory and metabolic processes in the cells of microscopic fungi with the participation of oxygen and water.

Interaction of aluminium with ROS produced by micromycetes. The surface charge of a protective aluminium oxide film plays an important role in its interaction with charged particles. We believe that the surface of aluminium in an aqueous solution containing hydroxide ions is negatively charged. This promotes the adsorption of electron acceptor molecules, including oxygen molecules, on the surface of a passive aluminium film, which are rapidly reduced on it.

If we assume that due to a local increase in pH, the protective passive film was dissolved and its clean surface was exposed, then aluminium will react rapidly with the ROS produced by micromycete cells. For example, it becomes possible for aluminium to interact with the superoxide anion radical released during the life of microscopic fungi, which can be represented by the scheme (8):

$$Al^o + O_2^{\bullet -} = [Al^o \cdots O_2^{\bullet -}]_{ads} = [Al^+(O_2^-)]^-. \quad (8)$$

The resulting surface adsorption complex undergoes hydrolysis with the formation of an OH^- ion and $Al(OH)_3$ by reactions (9)–(11):

$$[Al^+(O_2^-)]^- + H_2O = [AlO(OH)] + OH^-, \quad (9)$$

$$[AlO(OH)] + H_2O = Al(OH)_3, \quad (10)$$

$$AlO(OH) + H_2O + OH^- = [Al(OH)_4]^-. \quad (11)$$

After dissolution of the protective film of aluminium with the formation of tetrahydroxoaluminate ions, they diffuse into the volume of a drop of liquid exudate, where

its further transformations are possible in close proximity to the mycelium of micromycetes.

Hydroxide ions and water molecules are able to penetrate and move in films of surface oxygen compounds of aluminium [107]. Studies [108, 109] have shown a significant effect on the rate of dissolution of aluminium in an alkaline medium of the diffusion factor - the delivery of OH^- ions to corroding metal. We believe that the development of pitting corrosion of aluminium in an aqueous medium with pH>7 is initiated due to the local enrichment of the surface with hydroxide ions. The nucleation and development of pitting on the aluminium surface proceeds primarily in defects in the passive oxide film due to the displacement of oxygen-containing aluminium compounds by aggressive OH^- anions followed by the interaction of the metal with ROS. The adsorption/chemisorption of the superoxide anion radical on the hole centres of the passive aluminium film components is possible. For example, the ability of the γ-AlO(OH) boehmite surface to stabilise ROS has been proven [110]. The superoxide anion radical $O_2^{\bullet-}$ stabilises on the defect-free boehmite surface, then, with the participation of water, the surface hydroperoxide (perhydroxyl) radical $HO_2^{\cdot}$ is formed according to reactions (12)–(14):

$$O_2^{\bullet-} + (H_2O)\text{-}AlO(OH) = HO_2^{\bullet} + (^-HO)\text{–}AlO(OH), \quad (12)$$

or

$$O_2^{\bullet-} + (H_2O)\text{–}AlO(OH) = (^{\bullet-}O\text{–}O)\text{-}AlO(OH) + H_2O, \quad (13)$$

$$(^{\bullet-}O\text{–}O)\text{–}AlO(OH) + H_2O = (HO\text{–}O)\text{-}AlO(OH) + OH^-. \quad (14)$$

During the life of microscopic fungi, as well as under the conditions of oxidative stress of micromycete cells, a certain amount of endogenous hydrogen peroxide in concentrations of 10^{-4}–10^{-6} M metabolically accumulates in the environment. In this case, its interaction with aluminium can occur according to the Fenton reaction. The formation of hydroxyl radicals (HO^-) will be initiated through electron transfer from Al^o to H_2O_2 according to schemes (15)–(17) [111]:

$$Al^o + 3H_2O_2 = Al^{3+} + 3[H_2O_2]^{\bullet-}, \quad (15)$$

$$3[H_2O_2]^{\bullet-} = 3OH^- + 3OH^{\bullet}, \quad (16)$$

$$Al^{3+} + 3OH^- = Al(OH)_3. \quad (17)$$

Our experiments confirmed that the decomposition of hydrogen peroxide begins after some time, during which the natural oxide layer dissolves. Thus, under the considered conditions, hydrogen peroxide is an intermediate product of oxygen activation reactions and undergoes heterogeneous decomposition, electrochemical transformation (conjugated oxidation and reduction reactions), or enzymatic decomposition. In an alkaline environment H_2O_2 turns into HO_2^- and then reduced to OH^- according to schemes (18)–(20):

$$Al^o + 4OH^- - 3e = [Al(OH)_4]^-, \quad (18)$$

$$H_2O_2 + 2e = 2OH^-, \quad (19)$$

in total:

$$2Al^o + 2OH^- + 3H_2O_2 = 2[Al(OH)_4]^-. \quad (20)$$

Now, a number of literary sources [112 – 115] report that in an aqueous solution it is possible to generate isomeric forms of the HOOH molecule, in particular, the oxywater molecule $[H_2O^+O^-]$ in the form of a zwitterion. The latter heterolytically dissociates with the release of a water molecule and a singlet oxygen atom O([↑↓][↑][↓]) or ^{1}D-oxene O[↑↓][↑↓][_], which exhibit high oxidising properties and mediate the decomposition of hydrogen peroxide itself. We do not rule out the possibility of the formation of such highly reactive molecules in the studied system. The formation of oxywater and singlet oxygen can probably be postulated in the general scheme of aluminium–ROS interactions.

In the overall process of aluminium biocorrosion, we propose to conditionally distinguish several stages [116–118]. *Aluminium biocorrosion induction stage*, during which the hydrolysis of the protective passive film occurs, leading to an impairment of its continuity and an increase in the permeability for water molecules. This becomes possible due to the presence of structural defects in the passive aluminium film that are impermeable to air oxygen, but open upon contact with liquid water, for example, due to the Rehbinder effect. Another possible reason for the destruction of the protective film is its chemical dissolution, which will occur locally in its most defective sites. This is facilitated by the formation of a liquid exudate with basic properties by micromycetes. At pH > 7, the

dissolution of aluminium oxide compounds occurs mainly with the formation of $[Al(OH)_4]^-$ ions[119, 120] and includes oxide hydration and dissolution of the formed aluminium hydroxide according to schemes (21)–(23):

$Al_2O_3 + H_2O = 2AlO(OH)$

or

$$Al_2O_3 + 3H_2O = 2Al(OH)_3, \quad (21)$$

$$AlO(OH) + H_2O + OH^- = [Al(OH)_4]^-, \quad (22)$$

$$Al(OH)_3 + OH^- = [Al(OH)_4]^-. \quad (23$$

According to [121], when aluminium hydroxide comes into contact with metallic aluminium, the so-called "rehydrolysis" of aluminium hydroxide can occur, leading to the formation of aluminium oxide according to reaction (24):

$$2Al(OH)_3 + 2Al = 2Al_2O_3 + 3H_2. \quad (24)$$

The resulting aluminium oxide is less permeable to water molecules than aluminium hydroxide. Defects that are opened upon contact with water are closed by a newly formed oxide, which significantly inhibits the biocorrosion of the metal.

At the induction stage [77–80], the Al–O–Al structural bridges are destroyed with the formation of Al–OH bonds; at the same time, the pH of the exudate formed by micromycetes increases, the value of which can reach up to 11. With a passive aluminium film thickness of 2–4 nm [76], 5–10 aluminium oxide layers can be located above the surface of a pure metal. The passive film localised at the boundaries of crystal grains will probably have the most defective structure [79].

Hydroxyl groups are able to diffuse from the "exudate-passive film" interface to the "passive film-aluminium" interface, forming structural hydroxides. The diffusion of OH groups is significantly accelerated with an increase in the number of defects in alumina [80]. When the OH-groups come into contact with metallic aluminium, aluminium hydroxide is "rehydrolysed" according to reaction (24). The resulting aluminium oxide will increase the thickness of the passive film and may be hydrolysed again. The intensification of the process will be facilitated by the destruction of the oxide coating.

In experiments, we noticed the formation of hydrogen and saturation of drops of liquid exudate adjacent to the surfaces of the samples with it (Fig. 9). If the rate of hydrogen formation is higher than the rate of its diffusion, the resulting hydrogen, accumulating under the oxide coating, can lead to its destruction [75]. The oxide coating is a significant obstacle to the formation of hydrogen, since the diffusion coefficient of hydrogen in the oxide is 10^{-13}–10^{-14} cm^2/s [122, 123]. In turn, the effective diffusion coefficient of OH^--groups in the oxide is much lower and amounts to ~10^{-17} cm^2/s [80]. The conditional end of the induction period is due to the fact that the hydrolysed passive film dissolves locally in the most defective sites, which leads to the intensification of biocorrosion.

Intensive aluminium biocorrosion stage. As the oxidation of the metal proceeds, point penetration defects and their number per unit surface increases. The resulting aluminium hydroxide covers most of the aluminium surface. In the process of aluminium oxidation, aluminium hydroxide micelles are formed in the zones of penetration defects, which do not prevent the transfer of water to the oxidising metal, fill the defect volume, and eventually emerge on the

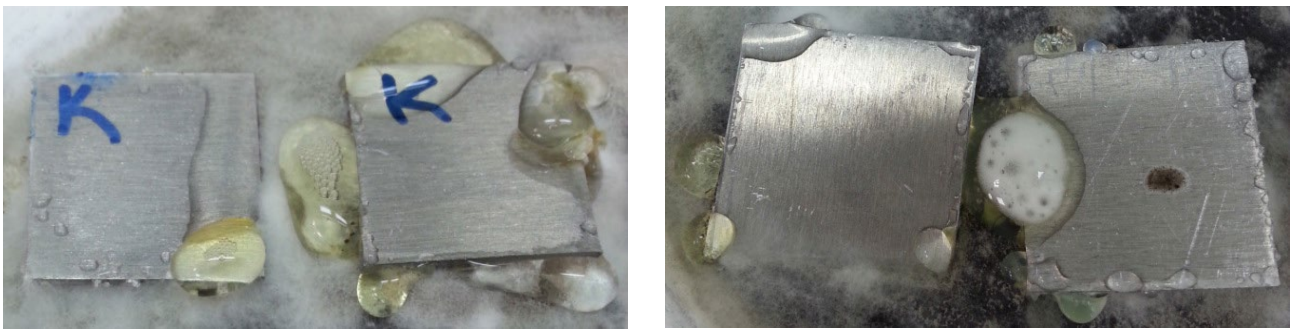

Fig. 9. The formation of hydrogen produced during the interaction of exudate with the D16T alloy at the sites of its contact with the lawn of micromycete mycelium.

aluminium surface. Further, this leads to the formation of a water-saturated gel, enveloping the corroding area of the surface of the metal sample.

The transfer of aluminium hydroxide is carried out mainly by ions $[Al(OH)_4]^-$ [118]. Mass transfer prevents the rapid accumulation of solid corrosion products on the aluminium surface and promotes an increase in the rate of biocorrosion. Over time, the gel-like aluminium hydroxide, enveloping the surface of the metal, is converted into its crystalline form. Over time, the gel ages: it loses water molecules, becomes structured, compacted, and loses the ability to pass water to the surface of the oxidised metal [77]. With a lack of hydroxide ions, a decrease in water permeability occurs due to an increase in the volume of corrosion products and structuring of the freshly formed hydroxide. These processes can be represented as a diagram: *micelles* $Al(OH)_3$ *→ water-saturated gel → structured gel → crystalline corrosion products*. From this moment, a slowdown in the overall rate of aluminium biocorrosion is observed. Intensive oxidation of the metal gradually fades.

pH change of the exudate during aluminium biocorrosion. We noticed that in the studied system, the pH value of the exudate formed at the metal–micromycete consortium boundary can either increase or decrease. It is known [124] that during the hydration of aluminium oxide, which forms a passive surface film, hydroxide ions are formed, which are bound to the metal surface in various ways. The formation of the surface charge is controlled by the adsorption of protons and hydroxide ions by active sites on the surface. The surface of aluminium hydroxide is amphoteric and, depending on the pH of the medium, can act as an acid or Bronsted base. It is known, that at a pH value less than the value corresponding to the zero charge point (ZCP), the surface is charged positively, and at a higher pH value, it is charged negatively. The ZCP value can vary from ~7 to ~10 depending on the type of aluminium oxide [124]. The decrease in exudate pH during the stage of intense biocorrosion of aluminium is associated with the dissolution of aluminium hydroxide, and the increase in pH is associated with the association of $Al(OH)_3$ into chains (polymerisation) [118], accompanied by the loss of OH^- according to reaction (25):

$$[Al(OH)_4]^- = Al(OH)_3 + OH^-. \quad (25)$$

These processes compete with each other. In turn, during the stage of biocorrosion initiation (3–5 days), the pH of the exudate can reach 8–9, which is associated with the formation of ROS by micromycete cells and their interaction with water and air oxygen. These observations were confirmed by us for a wide range of metals [125, 126].

Finishing stages of biocorrosion. The process of biocorrosion ends with the depletion of the nutrient medium and the termination of the life of micromycetes. In our experiments, after at

a b

Fig. 10. Biocorrosion products of the alloy: gel and jelly at the sites of exudate formation (a); crystalline corrosion products (b)

least ten months of exposure, complete depletion of the nutrient medium was observed. The products of aluminium biocorrosion successively turned from a gel (Fig. 10) into multi-coloured crystalline formations of irregular shape (Fig. 11). The surface of the samples, which was in direct contact with the lawn of micromycetes, was subjected to significant damage (Fig. 12).

Assessment of corrosion damage. Corrosion damage develops according to the mechanism of pitting corrosion, turning into ulcer corrosion, and is localised at the sites of contact of aluminium with exudate produced by micromycetes. After 10 months of exposure, the entire surfaces of the samples, which were in close contact with the mycelium of the consortium of microscopic fungi, were subject to corrosion damage. Characteristic features of the final stage of biocorrosion of aluminium alloys are deep ulcers (up to 2–3 mm) and cavities of various shapes filled with corrosion products (Figs. 11, 12).

Along with white and brown corrosion products in the form of irregularly shaped clusters, we observed an insignificant amount of light blue corrosion products characteristic of copper compounds (Fig. 13).

The results of X-ray phase analysis of the corrosion products of the D16T sample, which were collected from different parts of the surface, are shown in Table 1. During the destruction of

a b

Fig. 11. Appearance of samples with corrosion products: (a) 3 months after the beginning of the experiment; (b) 10 months after the start of the experiment

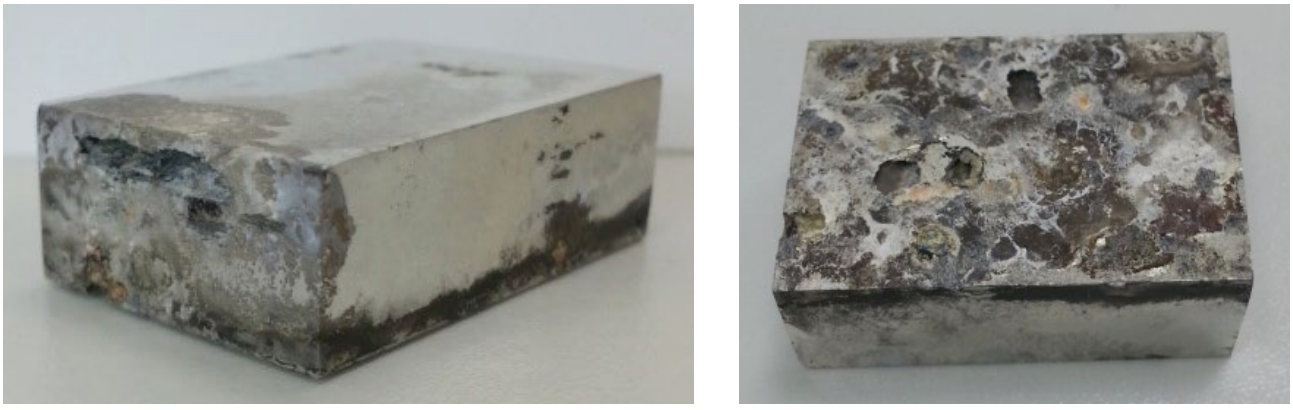

a b

Fig. 12. Appearance of the sample without corrosion products during the final stages of the experiment (10 months): lateral edges of the sample (a) (subsurface corrosion is clearly visible); surface in direct contact with the lawn of a micromycete consortium (b)

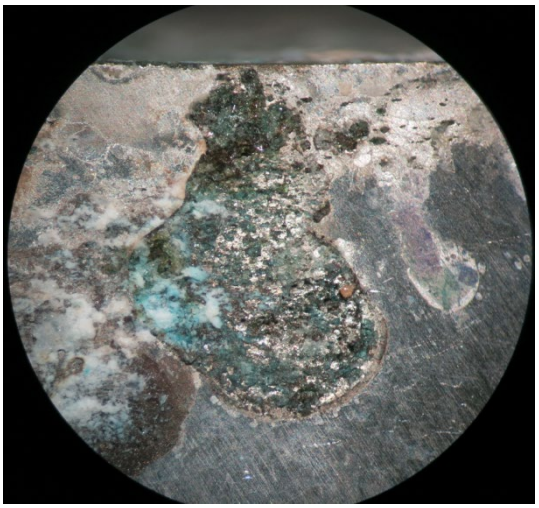

Fig. 13. Products of copper corrosion on the sample surface

the material under the influence of micromycetes, we found some oxygen compounds of aluminium in its corrosion products: γ-$Al(OH)_3$, α-AlO(OH), $5Al_2O_3 \cdot H_2O$ [120, 127, 128], copper and magnesium.

EDS analysis confirmed the presence of aluminium, copper, and magnesium oxygen compounds in the corrosion products [121, 129]. The results of the EDS analysis of the corrosion products of the D16T alloy sample collected from different parts of the sample surface are shown in Fig. 14. Phosphorus, sulphur and nitrogen were recorded in addition to oxygen among non-metals. In our opinion, the sources of these non-metals are the remains of cells of microscopic fungi and elements of the nutrient medium.

At the initial stage, local selective corrosion is observed on a small area, which intensively spreads deep into the metal along the grain boundaries. After, local corrosion in the form of spots spreads over the surface of the samples. Observations using an electron microscope made it possible to detect the presence of centres of intergranular corrosion (Fig. 15). The depth of corrosion damage in some areas of the surface reached 1.5–2.0 mm. A corrosive medium formed as a result of the activity of microscopic fungi and containing ROS and hydroxide ions entered deep into the metal and destroyed the outer grain boundaries of the D16T alloy. There was a fragmentary destruction of the grains. In this case, the grain boundary material acted as an anode to the copper-rich grains that are the cathode regions.

Microstructural studies of the samples showed the presence of areas of biocorrosion damage under the metal's surface. Subsurface corrosion starts at the surface of the metal and spreads deeper. The mycelium of microscopic fungi can easily penetrate into the formed cavities in the alloy, which contribute to the deepening of the process.

Table 1. Data of X-ray structural analysis of corrosion products of the D16T alloy

Location of sites (no. 1, no. 2) on the surface of the sample with corrosion products for which X-ray phase analysis was performed	Surface area number	2θ, grad	*d*, nm	*I*, %	Phase
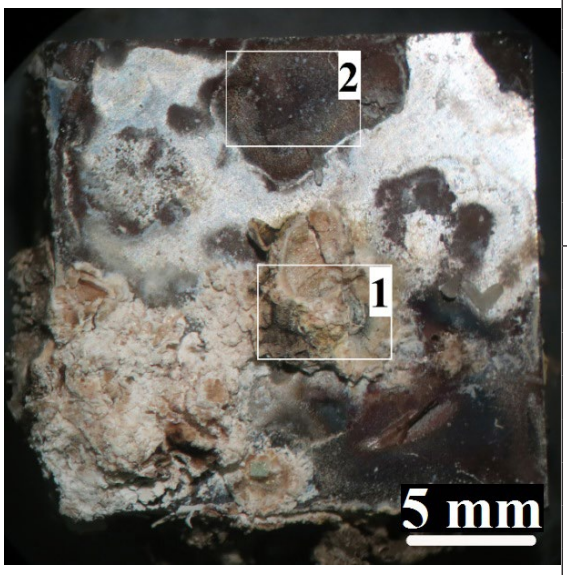	1	38.58	2.3336	100	Al
		40.2	2.2432	12.35	γ-$Al(OH)_3$
		43.54	2.0785	37.18	Al
		44.8	2.0230	58.70	γ-$Al(OH)_3$
		0.64	1.8025	16.97	γ-$Al(OH)_3$
		65.18	1.4312	15.46	Al
	2	35.22	2.5481	9.16	AlO(OH)
		36.9	2.4358	12.07	γ-$Al(OH)_3$
		38.69	2.3278	45.20	$5Al_2O_3 \cdot H_2O$
		40.26	2.2400	9.60	γ-$Al(OH)_3$
		44.94	2.0170	100	Al
		50.7	1.8005	15.13	γ-$Al(OH)_3$
		65.28	1.4293	51.96	Al
		78.3	1.2205	22.15	Al

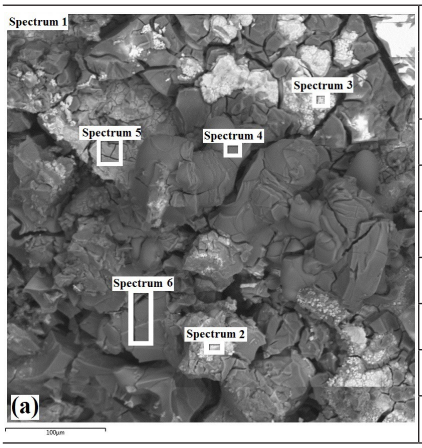

Element	Chemical composition in the site (a) of the surface, %					
	Spectrum 1	Spectrum 2	Spectrum 3	Spectrum 4	Spectrum 5	Spectrum 6
Al	25.27	9.97	20.22	26.51	23.54	11.07
Cu	9.98	65.55	2.22	0.95	7.67	63.98
Mg	0.3	0	0	0.57	0.28	0
O	53.46	22.56	63.16	66.18	46.5	55.7
P	2.06	0.73	1.29	0.71	3.54	1.05
S	5.08	1.18	8.82	1.16	13.59	0.89
N	3.84	0	4.29	3.86	4.88	0

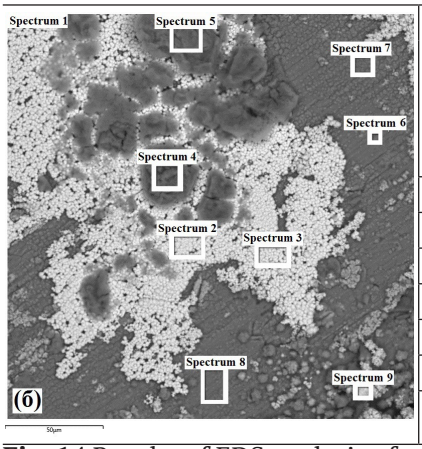

Element	Chemical composition in the site (b) of the surface, %								
	Spectrum 1	Spectrum 2	Spectrum 3	Spectrum 4	Spectrum 5	Spectrum 6	Spectrum 7	Spectrum 8	Spectrum 9
Al	32.87	0.7	0.54	9.65	9.11	67.17	59.18	63.66	2.81
Cu	35.21	89.43	90.57	4.81	3.74	3.54	4.44	3.86	77.67
Mg	1.35	0	0	1.95	1.85	1.3	1.38	1.42	0.92
O	20.82	7.13	6.54	51.24	53.7	21.67	25.40	22.72	12.24
P	3.05	0.3	0.26	9.94	9.29	2.1	2.85	2.91	2.01
S	0.79	0.87	0.68	0.87	1.0	0.39	1.0	0.74	0.78
N	1.98	0.97	0.98	3.84	3.91	1.49	2.35	1.99	1.38

Fig. 14 Results of EDS analysis of corrosion products in sites (a) and (b) on the sample surface

The presence of copper and magnesium compounds in the biocorrosion products of the D16T alloy can be explained by component-selective corrosion of the alloy and selective etching of aluminium from its structure. A more intense destruction of aluminium occurred in the surface layers of D16T. The interaction of copper and magnesium with ROS at pH>7 is also thermodynamically possible. This was confirmed by the EDS analysis of corrosion products studied on a transverse section of the sample (Table 1).

We proposed that the oxidation of copper in an alkaline medium is realised with the formation of oxygen compounds of copper according to schemes (26)-(28):

$$2\,Cu + 2OH^- - 2e = Cu_2O + H_2O, \quad (26)$$

$$Cu_2O + 2OH^- - 2e = 2CuO + H_2O, \quad (27)$$

$$Cu_2O + 2OH^- + H_2O - 2e = 2Cu(OH)_2. \quad (28$$

Intergranular corrosion. The analysis of literature data shows that the driving force of the IGC is the difference in electrochemical potentials that occurs at the matrix/particle interface (aluminium solid solution/second phase), the value of which, in the general case, is the higher, the less coherent the interface is and the larger the size particles [130].

The intensity and depth of IGC depend on the structure of the matrix, primarily on the length and structure of grain and subgrain boundaries [131]. Since the D16T alloy is located at the boundary of the (α + S) and (α + S + θ) regions, two types of strengthening particles can be distinguished in it – θ (Al_2Cu) and S (Al_2MgCu), the polarisation of which is different in relation to the matrix: the θ phase is the cathode in relation to the matrix, and the S phase is the anode.

The phase of Al_2Cu intermetallic compound is distinguished by grain boundaries, which are unstable and selectively decompose due to electrochemical heterogeneity. From the intermetallic compound Al_2Cu aluminium can selectively pass into the solution and the copper forms irregularly shaped conglomerates. The surface becomes porous, cavities of various configurations and depths are formed (Figs. 15, 16).

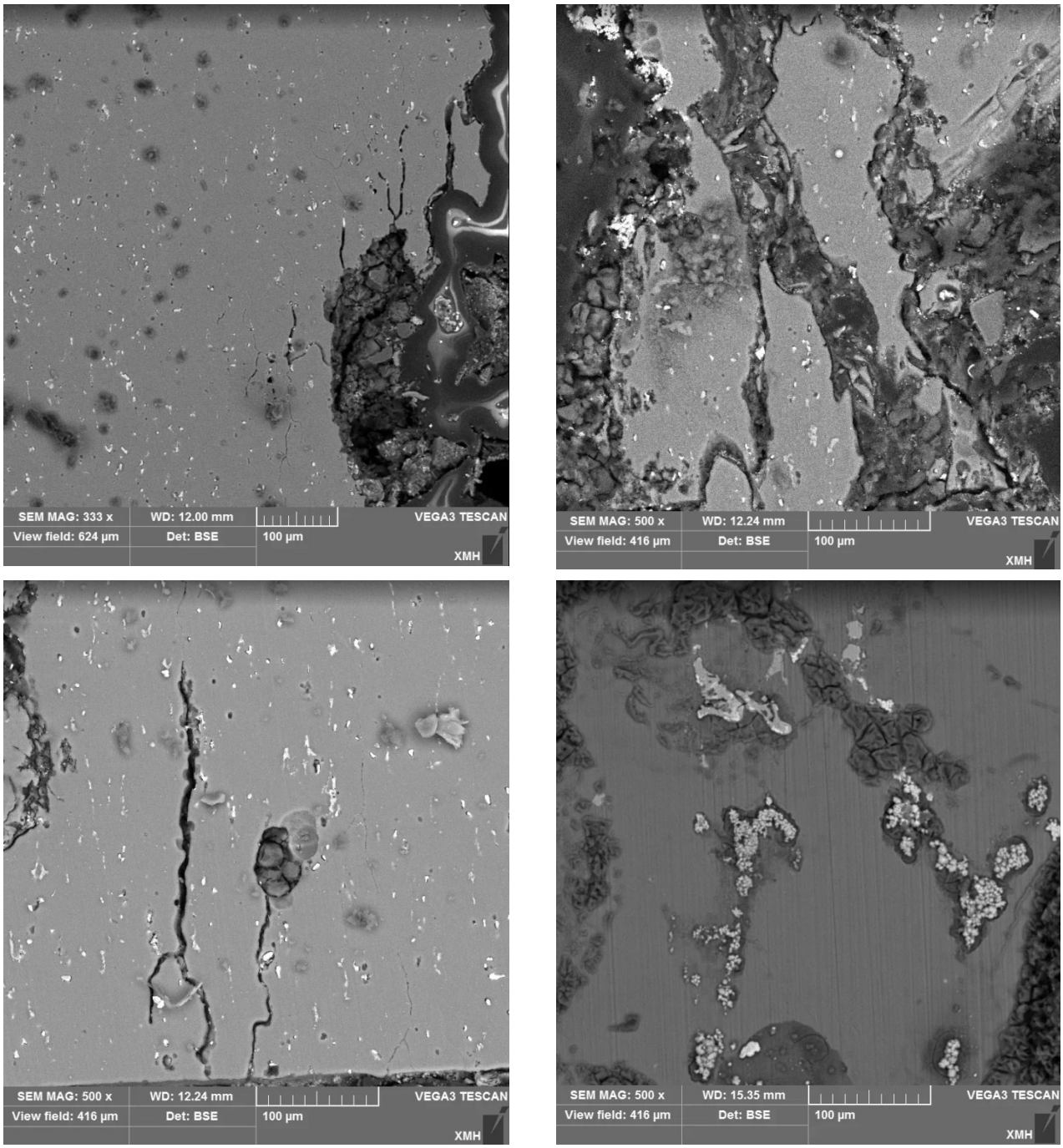

Fig. 15. Microstructures of different sections of the surface of a lateral section of a sample with foci of intergranular corrosion

Subsequently, copper also undergoes destruction, as evinced by the presence of its oxidation products.

The process of dissolution of the S phase is more complicated. First, it dissolves according to the anode mechanism, losing aluminium and magnesium ions. This leads to a change in the chemical composition of the phase, and it becomes a cathode in relation to the matrix, with a corresponding change in the mechanism of its chipping [130].

Based on the obtained data, it can be concluded that the IGC of the D16T alloy under the influence of microscopic fungi is due to the synergistic effect of structural and phase factors. Corrosion lesions are characterised by their great depth and branching. This may be due to the separation of phases along the boundaries of subgrains and the

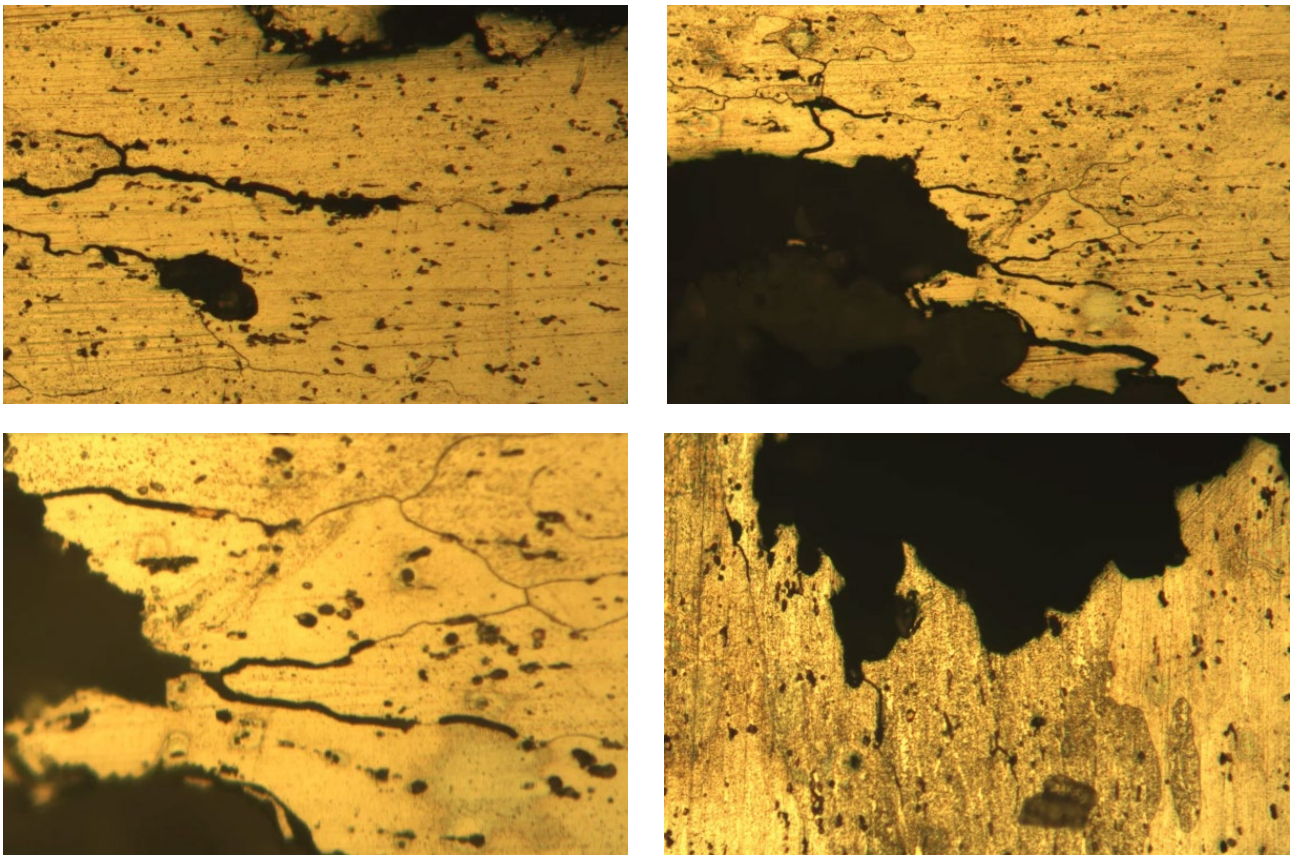

Fig. 16. Foci of intergranular corrosion of samples

emergence of a greater driving force of corrosion (difference in electrochemical potentials). Along with this, relatively narrow, but very deep channels of corrosion lesions are observed, which merge into continuous corrosion centres in the form of ulcers. This pattern may be due to the decomposition of the solid solution, which leads to the formation of large particles of stable S and θ phases in the recrystallised regions [132, 133].

Classical methods of corrosion protection, such as the use of organic inhibitors or coatings based on polymeric materials, become ineffective under conditions of microscopic fungi development. Much more often, experts offer methods of inhibiting, rather than combating biocorrosion. The tactics of combating the biocorrosion of metals under the influence of micromycetes should take into account the peculiarities of the biochemical mechanisms of the functioning of microorganisms. Only by knowing the mechanisms of interaction in the "microorganism - metal" system is it possible to create effective ways to protect metals from biocorrosion.

The formation and release of reactive oxygen species by micromycetes into the external environment is one of the factors of biocorrosion. Hyperproduction of ROS may be a consequence of oxidative stress in micromycetes. This may be caused by an impairment of the natural "redox status" of microscopic fungal cells that are in direct contact with the metal surface. The presence of water contributes to the conversion of ROS into their most stable and "long-lived" forms, which either initiate the biocorrosion of duralumin and its alloys themselves, or trigger a cascade of reactions involving hydroxide ions.

Model systems show that the surface of an aluminium alloy in contact with micromycete consortiums is subjected to global destruction, which is unacceptable when operating equipment or products under the influence of micromycetes. Based on a detailed study of the mechanism of occurrence and development of biocorrosion of duralumin under the influence of microscopic fungi, effective methods of protection against biocorrosion will be developed.

4. Conclusions

During the vital activity of microscopic fungi, reactive oxygen species that initiate the biocorrosion of the D16T alloy are formed. The initial stage of biocorrosion is due to the hydrolysis of the protective passive aluminium film. During the stage of intense biocorrosion, oxygen-containing aluminium compounds in the form of a water-saturated gel are formed. Further, this corrosion product is accumulated and its water permeability decreases. The gel undergoes "ageing" and turns into crystalline products. The conidia and hyphae of microscopic fungi adhere, mechanically attach to the surface of the metal and penetrate into the surface layers and deep into the metal, causing its corrosion damage in the form of pitting, ulcers, and cavities. The initiation of metal biocorrosion is a consequence of the hyperproduction of reactive oxygen species by micromycete cells as a result of oxidative stress. This may be their defensive strategy aimed at destroying xenobiotic material.

The development of intergranular and pitting corrosion of the D16T alloy under the action of micromycetes occurs at the sites of contact with exudate, which is locally enriched in hydroxide ions due to the cascade of reactions involving ROS. The nucleation and development of pitting on the surface of duralumin occurs in the defects of the passive oxide film due to the displacement of oxygen-containing surface compounds of aluminium and their interaction with corrosive OH^- anions and ROS. Hydrogen peroxide, as an intermediate product of the metabolism of micromycetes, on the surface of the D16T alloy can participate in the Fenton process or decompose heterogeneously, also provoking the development of aluminium biocorrosion.

The ultimate goal of research into the microbial corrosion of metals is the development of molecular tools aimed at diagnosing the occurrence, studying the mechanisms and rates of metal biocorrosion. This will allow the most effective strategies for protecting materials from biodegradation to be implemented. A systematic biological approach is required, including innovative methods for the isolation and characterisation of corrosive strains of microscopic fungi; conducting functional genomic studies; the investigation of the functioning of microbial communities and dynamically developing relationships with environments; and the study of unique metabolites that are the end points of specific cellular processes.

For the determination of diagnostic signs of biocorrosion processes in metals, it is necessary to carry out a systematic study of the unique chemical and biochemical processes occurring in living cells, including the study of their low molecular weight metabolic profiles.

The study of metal corrosion mechanisms involving microbial communities will lead to new strategies for protection against biocorrosion. Our progress in understanding the mechanisms of corrosion of metals under different microbiomes is at an embryonic stage, but interdisciplinary electrochemical, microbiological and molecular tools will enable rapid progress in this area.

Author contributions

Belov D. V. – scientific leadership, research concept, methodology development, text writing, final conclusions. Belyaev S. N. – conducting experimental studies, writing a literature review and text editing.

Conflict of interests

The authors declare that they have no known competing financial interests or personal relationships that could have influenced the work reported in this paper.

References

1. Kolesnikova N. N., Lukanina Yu. K., Khvatov A. V. Biological corrosion of metal structures and protection against it. *Bulletin of the Kazan Technological University*. 2013;16(1): 170–174. (In Russ., abstract in Eng.). Available at: https://www.elibrary.ru/item.asp?id=18726011

2. Lekbach Y., Liu T., Li Y., Moradi M., Dou W., Xu D., Smith J. A., Lovley D. R. Microbial corrosion of metals: The corrosion microbiome. *Advances in Microbial Physiology*. 2021;78: 317–390. https://doi.org/doi:10.1016/bs.ampbs.2021.01.002

3. Tang H. Y., Yang C., Ueki T., Pittman C. C., Xu D., Woodard T. L., Holmes D. E., Gu T., Wang F., Lovley D. R. Stainless steel corrosion via direct iron-to-microbe electron transfer by Geobacter species. *The ISME Journal: Multidisciplinary Journal of Microbial Ecology*. 2021;15: 3084–3093. https://doi.org/10.1038/s41396-021-00990-2

4. Tang H. Y., Holmes D. E., Ueki T., Palacios P. A., Lovley D. R. Iron corrosion via direct metal-microbe

electron transfer. *mBio*. 2019;10(3): e00303-19. https://doi.org/10.1128/mBio.00303-19

5. Deutzmann J. S., Sahin M., Spormann A. M. Extracellular enzymes facilitate electron uptake in biocorrosion and bioelectrosynthesis. *mBio*. 2015;6(2): e00496-15. https://doi.org/10.1128/mbio.00496-15

6. Costerton J. W., Geesey G. G., Cheng K. J. How bacteria stick. *Scientific American*. 1978;238(1): 86–95. https://doi.org/10.1038/scientificamerican0178-86

7. Li X., Duan J., Xiao H., Li Y., Liu H., Guan F., Zhai X. Analysis of bacterial community composition of corroded steel immersed in sanya and xiamen seawaters in China via method of illumina MiSeq Sequencing.. *Frontiers in Microbiology*. 2017;8: 1737. https://doi.org/10.3389/fmicb.2017.01737

8. Cetin D., Aksu M. L. Corrosion behavior of low-alloy steel in the presence of *Desulfotomaculum* sp. *Corrosion Science*. 2009;51(8): 1584–1588. https://doi.org/10.1016/j.corsci.2009.04.001

9. Wikieł A. J., Datsenko I., Vera M., Sand W. Impact of *Desulfovibrio alaskensis* biofilms on corrosion behaviour of carbon steel in marine environment. *Bioelectrochemistry*. 2014;97: 52–60. https://doi.org/10.1016/j.bioelechem.2013.09.008

10. Zhang P., Xu D., Li Y., Yang K., Gu T. Electron mediators accelerate the microbiologically influenced corrosion of 304 stainless steel by the *Desulfovibrio vulgaris* biofilm. *Bioelectrochemistry*. 2015;101: 14–21. https://doi.org/10.1016/j.bioelechem.2014.06.010

11. McBeth J. M., Emerson D. In situ microbial community succession on mild steel in estuarine and marine environments: Exploring the role of iron-oxidizing bacteria. *Frontiers in Microbiology*. 2016; 7. https://doi.org/10.3389/fmicb.2016.00767

12. Dinh H. T., Kuever J., Mußmann M., Hassel A. W., Stratmann M., Widdel F. Iron corrosion by novel anaerobic microorganisms. *Nature*. 2004;427(6977): 829–832. https://doi.org/10.1038/nature02321

13. Beech I. B., Gaylarde C. C. Adhesion of *Desulfovibrio desulfuricans* and *Pseudomonas fluorescens* to mild steel surfaces. *Journal of Applied Bacteriology*. 1989;67(2): 201–207. https://doi.org/10.1111/ j.1365-2672.1989.tb03396.x

14. Zottola E. A. Characterization of the attachment matrix of *Pseudomonas fragi* attached to non-porous surfaces. *Journal of Bioadhesion and Biofilm Research*. 1991;5(1-2): 37–55. https://doi.org/10.1080/08927019109378227

15. Siqueira V. M., Lima, N. Biofilm formation by filamentous fungi recovered from a water system. *Journal of Mycology*. 2013; Article ID 152941: 1–9. https://doi.org/10.1155/2013/152941

16. Fox E. P., Singh-Babak S. D., Hartooni N., Nobile C. J. Biofilms and antifungal resistance. *Antifungals: From Genomics to Resistance and the Development of Novel Agents*. 2015; 71–90. https://doi.org/10.21775/9781910190012.04

17. Müller F.-M. C., Seidler M., Beauvais A. *Aspergillus fumigatus* biofilms in the clinical setting. *Medical Mycology*. 2011;49(S1): S96–S100. https://doi.org/10.3109/13693786.2010.502190

18. Reichhardt C., Ferreira J. A. G., Joubert L.-M., Clemons K. V., Stevens D. A., Cegelski L. Analysis of the *Aspergillus fumigatus* biofilm extracellular matrix by solid-state nuclear magnetic resonance spectroscopy. *ASM Journals. Eukaryotic Cell*. 2015;14(11): 1064–1072. https://doi.org/10.1128/EC.00050-15

19. Donlan R. M. Biofilms: Microbial life on surfaces. *Emerging Infectious Diseases*. 2002;8(9): 881–890. https://doi.org/10.3201/eid0809.020063

20. Gorbushina A. A., Panina L. K. Adhesion of micromycete conidia to polymeric materials. *Mycology and Phytopathology*. 1992;26(5): 372–377. (In Russ.)

21. Kalinina I. G., Gumargalieva K. Z., Kuznetsova O. N., Zaikov G. E. Interrelation of adhesion of conidia of the microscopic fungus Trichoderma viride with the electrochemical properties of metals. *Bulletin of the Kazan Technological University*. 2012;15(12): 115–118. (In Russ., abstract in Eng.). Available at: https://www.elibrary.ru/item.asp?id=17846266

22. Joubert L.-M., Ferreira J. A., Stevens D. A., Nazik H., Cegelski L. Visualization of *Aspergillus fumigatus* biofilms with scanning electron microscopy and variable pressure-scanning electron microscopy: A comparison of processing techniques. *Journal of Microbiological Methods*. 2017;132: 46–55. https://doi.org/10.1016/j.mimet.2016.11.002

23. González-Ramírez A.I., Ramírez-Granillo A., Medina-Canales M. G., Rodríguez-Tovar A. V., Martínez-Rivera M. A. Analysis and description of the stages of *Aspergillus fumigatus* biofilm formation using scanning electron microscopy. *BMC Microbiology*. 2016;16, 243. https://doi.org/10.1186/s12866-016-0859-4

24. Villena G. K., Fujikawa T., Tsuyumu S., Gutiérrez-Correa M. Structural analysis of biofilms and pellets of *Aspergillus niger* by confocal laser scanning microscopy and cryo scanning electron microscopy. *Bioresource Technology*. 2010;101(6): 1920–1926. https://doi.org/10.1016/j.biortech.2009.10.036

25. Denkhaus E., Meisen S., Telgheder U., Wingender J. Chemical and physical methods for characterisation of biofilms. *Microchimica Acta*. 2007;158(1-2): 1–27. https://doi.org/10.1007/s00604-006-0688-5

26. Beech I. B., Sunner J. A., Hiraoka K. Microbe–surface interactions in biofouling and biocorrosion processes. *International Microbiology*. 2005;8: 157–168. PMID: 16200494. https://doi.org/10.2436/IM.V8I3.9522

27. Beech I. B., Sunner J. Biocorrosion: towards understanding interactions between biofilms and metals. *Current Opinion in Biotechnology*. 2004;15(3): 181–186. https://doi.org/10.1016/j.copbio.2004.05.001

28. Yang S. L., Chung K. R. The NADPH-oxidase-mediated production of hydrogen peroxide (H_2O_2) and resistance to oxidative stress in the necrotrophic pathogen *Alternaria alternata* of citrus. *Molecular Plant Pathology*. 2012;13(8): 900–914. https://doi.org/10.1111/j.1364-3703.2012.00799.x

29. Gessler N. N., Averyanov A. A., Belozerskaya T. A. Reactive oxygen species in the regulation of fungal development (Review). *Biochemistry*. 2007;72(10): 1091–1109. https://doi.org/10.1134/s0006297907100070

30. Gamaley I. L., Klyubin N. N. The role of hydrogen peroxide as a second messenger. *Tsitologiya*. 1996;38(12): 1242-1247. Available at: https://www.elibrary.ru/item.asp?id=14933936

31. Barsukova M. E., Veselova I. A., Shekhovtsova T. N. Main methods and approaches to the determination of markers of oxidative stress - organic peroxide compounds and hydrogen peroxide. *Journal of Analytical Chemistry*. 2019;74(5): 425-436. https://doi.org/10.1134/S1061934819020035

32. Hansberg W., Aguirre J. Hyperoxidant states cause microbial cell differentiation by cell isolation from dioxygen. *Journal of Theoretical Biology*. 1990;142(2): 201–221. PMID: 2352433. https://doi.org/10.1016/s0022-5193(05)80222-x

33. Sideri M., Georgiou C. D. Differentiation and hydrogen peroxide production in *Sclerotium rolfsii* are induced by the oxidizing growth factors, light and iron. *Mycologia*. 2000;92(6): 1033–1042. https://doi.org/10.2307/3761468

34. Tkachuk V. A., Tyurin-Kuzmin P. A., Belousov V. V., Vorotnikov A. V. Hydrogen peroxide as a new secondary Messenger. *Biological Membranes*. 2012;29(1–2): 21–37. (In Russ., abstract in Eng.). Available at: https://istina.msu.ru/media/publications/articles/300/3a4/1513469/BMM0021.pdf

35. Zúñiga-Silva J. R., Chan-Cupul W., Kuschk P., Loera O., Aguilar-López R., Rodríguez-Vázquez R. Effect of Cd^{+2} on phosphate solubilizing abilities and hydrogen peroxide production of soil-borne micromycetes isolated from *Phragmites australis*-rhizosphere. *Ecotoxicology*. 2015;25(2): 367–379. https://doi.org/10.1007/s10646-015-1595-5

36. Zhang J., Miao Y., Rahimi M. J., Zhu H., Steindorff A., Schiessler S., Cai F., PangG., Chenthamara K., Xu Y., Kubicek C. P., Shen Q., Druzhinina I. S. Guttation capsules containing hydrogen peroxide: an evolutionarily conserved NADPH oxidase gains a role in wars between related fungi. *Environmental Microbiology*. 2019;21(8): 2644–2658 https://doi.org/10.1111/1462-2920.14575

37. Stosz S. K., Fravel D. R., Roberts D. P. In vitro analysis of the role of glucose oxidase from Talaromyces flavus in biocontrol of the plant pathogen *Verticillium dahliae*. *Applied and Environmental Microbiology*. 1996;62(9): 3183–3186. https://doi.org/10.1128/aem.62.9.3183-3186.1996

38. Murray F. R., Llewellyn D. J., Peacock W. J., Dennis E. S. Isolation of the glucose oxidase gene from *Talaromyces flavus* and characterisation of its role in the biocontrol of *Verticillium dahliae*. *Current Genetics*. 1997;32(5): 367–375. https://doi.org/10.1007/s002940050290

39. Yang C.-A., Cheng C.-H., Lo C.-T., Liu S.-Y., Lee J.-W., Peng K.-C. A Novell-Amino Acid Oxidase from *Trichoderma harzianum* ETS 323 Associated with Antagonism of *Rhizoctonia solani*. *Journal of Agricultural and Food Chemistry*. 2011;59(9): 4519–4526. https://doi.org/10.1021/jf104603w

40. Smirnova I. P., Karimova E. V., Shneider Y. A. Antibacterial Activity of L-Lysine-α-Oxidase from the Trichoderma. *Bulletin of Experimental Biology and Medicine*. 2017;163(6): 777–779. https://doi.org/10.1007/s10517-017-3901-0

41. Heller J., Tudzynski P. Reactive oxygen species in phytopathogenic fungi: signaling, development, and disease. *Annual Review of Phytopathology*. 2011;49(1): 369–390. https://doi.org/10.1146/annurev-phyto-072910-095355

42. Mentges M., Bormann J. Real-time imaging of hydrogen peroxide dynamics in vegetative and pathogenic hyphae of *Fusarium graminearum*. *Scientific Reports*. 2015;5(1), 14980: 1–10. https://doi.org/10.1038/srep14980

43. Eichlerová I., Homolka L., Lisá L., Nerud F. The influence of extracellular H_2O_2 production on decolorization ability in fungi. *Journal of Basic Microbiology*. 2006;46(6): 449–455. https://doi.org/10.1002/jobm.200610064

44. Zhao J., Janse B. J. H. Comparison of H_2O_2-producing enzymes in selected white rot fungi. *FEMS Microbiology Letters*. 1996;139(2-3): 215–221. https://doi.org/10.1111/j.1574-6968.1996.tb08205.x

45. Wiberth C.-C., Casandra A.-Z. C., Zhiliang F., Gabriela H. Oxidative enzymes activity and hydrogen peroxide production in white-rot fungi and soil-borne micromycetes co-cultures. *Annals of Microbiology*. 2019;69: 171–181. https://doi.org/10.1007/s13213-018-1413-4

46 Zhao Y., Li J., Chen Y., Hang H. Response to oxidative stress of *Coriolus versicolor* induced by exogenous hydrogen peroxide and paraquat. *Annals of Microbiology*. 2009;59(2): 221–227. https://doi.org/10.1007/bf03178320

47. Hansel C. M., Zeiner C. A., Santelli C. M., Webb S. M. Mn(II) oxidation by an ascomycete fungus is linked to superoxide production during asexual

reproduction. *Proceedings of the National Academy of Sciences*. 2012;109(31): 12621–12625. https://doi.org/10.1073/pnas.1203885109

48. Hayyan M., Hashim M. A., AlNashef I. M. Superoxide Ion: Generation and Chemical Implications. *Chemical Reviews*. 2016;116(5): 3029–3085. https://doi.org/10.1021/acs.chemrev.5b00407

49. Winterbourn C. C. Biological chemistry of superoxide radicals. *ChemTexts (The Textbook Journal of Chemistry)*. 2020;6(1): 7. https://doi.org/10.1007/s40828-019-0101-8

50. Janik I., Tripathi G. N. R. The nature of the superoxide radical anion in water. *The Journal of Chemical Physics*. 2013;139(1): 014302-1–014302-7. https://doi.org/10.1063/1.4811697

51. Belov D. V., Chelnokova M. V., Kalinina A. A., Sokolova T. N., Smirnov V. F., Kartashov V. R. Active oxygen species in metal corrosion. *Corrosion: Materials, Protection*. 2011;3: 19–26. (In Russ.). Available at: https://www.elibrary.ru/item.asp?id=16317997

52. Belov D. V., Chelnokova M. V., Sokolova T. N., Smirnov V. F., Kalinina A. A., Kartashov V. R. Generation of superoxide radical anion by micromycetes and its role in metal corrosion. *ChemChemTech*. 2011;54(10): 133–136. (In Russ.). Available at: https://www.elibrary.ru/item.asp?id=16547211

53. De Grey A. D. N. J. $HO_2^{\bullet}$: The Forgotten Radical. *DNA and Cell Biology*. 2002;21(4): 251–257. https://doi.org/10.1089/104454902753759672

54. Bielski B. H. J., Allen A. O. Mechanism of the disproportionation of superoxide radicals. *Journal of Physical Chemistry*. 1977;81(11): 1048–1050. https://doi.org/10.1021/j100526a005

55. Xu W., Yu F., Yang L., Zhang B., Hou B., Li Y. Accelerated corrosion of 316L stainless steel in simulated body fluids in the presence of H_2O_2 and albumin. *Materials Science and Engineering: C*. 2018;92: 11–19. https://doi.org/10.1016/j.msec.2018.06.023

56. Yu F., Addison O., Davenport A. J. A synergistic effect of albumin and H_2O_2 accelerates corrosion of Ti6Al4V. *Acta Biomaterialia*. 2015;26: 355–365. https://doi.org/10.1016/j.actbio.2015.07.046

57. Miyazawa T., Terachi T., Uchida S., Satoh T., Tsukada T., Satoh Y., Wada Y., Hosokawa H. Effects of hydrogen peroxide on corrosion of stainless steel, (V) characterization of oxide film with multilateral surface analyses. *Journal of Nuclear Science and Technology*. 2006;43(8): 884–895. https://doi.org/10.1080/18811248.2006.9711173

58. Dong C., Yuan C., Bai X., Li J., Qin H., Yan X. Coupling mechanism between wear and oxidation processes of 304 stainless steel in hydrogen peroxide environments. *Scientific Reports*. 2017;7(1): 2327. https://doi.org/10.1038/s41598-017-02530-5

59. Singh A., Chaudhary V., Sharma A. Electrochemical studies of stainless steel corrosion in peroxide solutions. *Portugaliae Electrochimica Acta*. 2012;30(2): 99–109. https://doi.org/10.4152/pea.201202099

60. Mabilleau G., Bourdon S., Joly-Guillou M. L., Filmon R., Baslé M. F., Chappard D. Influence of fluoride, hydrogen peroxide and lactic acid on the corrosion resistance of commercially pure titanium. *Acta Biomaterialia*. 2006;2(1): 121–129. https://doi.org/10.1016/j.actbio.2005.09.004

61. Furiya-Sato S., Fukushima A., Mayanagi G., Sasaki K., Takahashi N. Electrochemical evaluation of the hydrogen peroxide- and fluoride-induced corrosive property and its recovery on the titanium surface. *Journal of Prosthodontic Research*. 2020;64(3): 307–312. https://doi.org/10.1016/j.jpor.2019.09.002

62. Yu F., Addison O., Davenport A. J. A synergistic effect of albumin and H_2O_2 accelerates corrosion of Ti6Al4V. *Acta Biomaterialia*. 2015;26: 355–365. https://doi.org/10.1016/j.actbio.2015.07.046

63. Been J., Tromans D. Titanium corrosion in alkaline hydrogen peroxide. *Corrosion*. 2000;56(8): 809–818. https://doi.org/10.5006/1.3280584

64. *Handbook of electrochemistry*. A. M. Sukhotin (Ed.). Leningrad: Chemistry Publ.; 1981. 488 p. (In Russ.)

65. Antonchenko V. Ya., Davydov A. S., Ilyin V. V. *Fundamentals of water physics*. AN Ukrainian SSR. Institute of Theoretical Physics. Kyiv: Naukova dumka Publ.; 1991. 672 p. (In Russ.)

66. *Handbook. Structure and corrosion of metals and alloys*: Atlas. Moscow: Metallurgy Publ.; 1989. 400 p.

67. Moon S.-M., Pyun S.-I. The formation and dissolution of anodic oxide films on pure aluminum in alkaline solution. *Electrochimica Acta*. 1999;44: 2445–2454. https://doi.org/10.1016/S0013-4686(98)00368-5

68. Davis G. D., Moshier W. C., Long G. G., Black D. R. Passive film structure of supersaturated Al-Mo alloys. *Journal of the Electrochemical Society*. 1991;138(11): 3194–3198. https://doi.org/10.1149/1.2085392

69. Nguyen L., Hashimoto T., Zakharov D. N., Stach E. A., Rooney A. P., Berkels B., Burnett T. L. Atomic-scale insights into the oxidation of aluminum. *ACS Applied Materials & Interfaces*. 2018;10(3): 2230–2235. https://doi.org/10.1021/acsami.7b17224

70. Hunter M. S., Fowle P. Natural and thermally formed oxide films on aluminum. *Journal of the Electrochemical Society*. 1956;103(9): 482–485. https://doi.org/10.1149/1.2430389

71. Gulbransen Earl A., Wysong W. S. Thin Oxide Films on Aluminum. *Journal of Physical Chemistry*. 1947;51(5): 1087–1103. https://doi.org/10.1021/j150455a004

72. Vargel C. *Corrosion of aluminium*. Hardbound: Elsevier; 2004. 700 p.

73. Gromov A. A., Il'in A. P., Foerter-Barth U., Teipel U. D. Effect of the passivating coating type, particle size, and storage time on oxidation and nitridation of aluminum powders. *Combustion, Explosion and Shock Waves*. 2006;42(2): 177–184. https://doi.org/10.1007/S10573-006-0036-4

74. Larichev M. N., Laricheva O. O., Leipunsky I. O., Pshechenkov P. A., Zhigach A. N., Kuskov M. L., Sedoy V. S. New "reactive" coatings for passivation surfaces of nanosized Al particles intended for energy use. *Khimicheskaya fizika*. 2006;25(10): 72–79. (In Russ.). Available at: https://www.elibrary.ru/item.asp?id=9295873

75. Deng Z. Y., Ferreira J. M. F., Tanaka Y., Ye J. Physicochemical mechanism for the continuous reaction of γ-Al_2O_3 modified Al powder with water. *Journal of the American Ceramic Society*. 2007;90(5): 1521–1526. https://doi.org/10.1111/j. 1551-2916.2007.01546.x

76. Fernandez A., Sanchez-Lopez J. C., Caballero A. Characterization of nanophase Al-oxide/Al powders by electron energy-loss spectroscopy. *Journal of Microscopy*. 1998;191: 212–220. https://doi.org/10.1046/j.1365-2818.1998.00355.x

77. Razavi-Tousi S. S., Szpunar J. A. Mechanism of corrosion of activated aluminum particles by hot water. *Electrochimica Acta*. 2014;127: 95–105. https://doi.org/10.1016/j.electacta.2014.02.024

78. Lozhkomoev A. S., Glazkova E. A., Bakina O. V., Lerner M. I., Gotman I., Gutmanas E. Y., Kazantsev S. O., Psakhie S. G. Synthesis of core-shell AlOOH hollow nanospheres by reacting Al nanoparticles with water. *Nanotechnology*. 2016;27(20): 205603 (7 pp). https://doi.org/10.1088/0957-4484/27/20/205603

79. Kanehira S., Kanamori S., Nagashima K., Saeki T., Visbal H., Fukui T. Controllable hydrogen release via aluminum powder corrosion in calcium hydroxide solutions. *Journal of Asian Ceramic Societies*. 2013;1: 296–303. https://doi.org/10.1016/j.jascer.2013.08.001

80. Bunker B. C., Nelson G. C., Zavadil K. R., Barbour J. C., Wall F. D., Sullivan J. P., Windisch C. F., Engelhardt M. H., Baer D. R. Hydration of passive oxide films on aluminum. *The Journal of Physical Chemistry B*. 2002;18(106): 4705–4713. https://doi.org/10.1021/jp013246e

81. Fateev Yu. F., Vrzhosek G. G., Antropov L. I. On the corrosion of aluminum in alkali solutions. *Bulletin of the Kiev Polytechnic Institute. Series: Chemical Engineering and Technology*. 1979;16: 60–63. (In Russ.). Available at: https://www.elibrary.ru/item.asp?id=17937682

82. Grigor'eva I. O., Dresvyannikov A. F. Corrosion and electrochemical behavior of aluminum in solutions of potassium and lithium hydroxides. *Bulletin of the Kazan Technological University*. 2012;15(14): 199–202. (In Russ., abstract in Eng.). Available at: https://www.elibrary.ru/item.asp?id=17937682

83. Grigoryeva I. O., Dresvyannikov A. F., Masnik O. Yu., Zakirov R. A. Electrochemical behavior of aluminum in solutions of ammonium hydroxide and sodium hydroxide. *Bulletin of the Kazan Technological University*. 2011;6: 72–78. (In Russ., abstract in Eng.). Available at: https://www.elibrary.ru/item.asp?id=16147047

84. Pyun S. I., Moon S. M. Corrosion mechanism of pure aluminium in aqueous alkaline solution. *Journal of Solid State Electrochemistry*. 2000;5(4): 267–272. https://doi.org/10.1007/s100080050203

85. Bryan J. M. *Aluminium and aluminium alloys in the food industry with special reference to corrosion and its prevention*. Department of Science and Industrial Research. Food Investigation Special Report. London: H. M. Stationery Office; 1948;50: p. 153.

86. Laptev A. B., Lutsenko A. N., Kurs M. G., Bukharev G. M. Experience studies of bio-corrosion of metals. *Theory and Practice of Corrosion Protection*. 2016;2(80): 36–57. (In Russ., absract in Eng.). Available at: https://www.elibrary.ru/item.asp?id=29311937

87. Nardy K., Johannes A.V. The dual role of microbes in corrosion. *The ISME Journal*. 2015;9(3): 542–551. https://doi.org/10.1038/ismej.2014.169

88. Smirnov V. F., Belov D. V., Sokolova T. N., Kuzina O. V., Kartashov V. R. Microbiological corrosion of aluminum alloys. *Applied Biochemistry and Microbiology*. 2008;44: 192–196. https://doi.org/10.1134/S0003683808020117

89. Belov D. V., Belyaev S. N., Maksimov M. V., Gevorgyan G. A. Research of corrosion fracture of D16T and AMg6 aluminum alloys exposed to microscopic fungi. *Voprosy Materialovedeniya*. 2021;3(107): 163–183. https://doi.org/10.22349/1994-6716-2021-107-3-163-183

90. Belov D. V., Chelnokova M. V., Sokolova T. N., Smirnov V. F., Kartashov V. R. On the role of reactive oxygen species in the initiation of corrosion of metals by microscopic fungi. *Korroziya: Materialy, Zashchita*. 2009;11: 43–48. (In Russ.). Available at: https://www.elibrary.ru/item.asp?id=13032869

91. Koval E. Z., Sidorenko L. P. *Microdestructors of industrial materials*. Kyiv: Naukova Dumka Publ.; 1989. 192 p. (In Russ.)

92. Sutton D. A, Fothergill A. W, Rinaldi M. G. Guide to clinically significant fungi. Baltimore: Williams & Wilkins; 1997. 471 p.

93. Berridge M. V., Herst P. M., Tan A. S. Tetrazolium dyes as tools in cell biology: New insights into their cellular reduction. *Biotechnology Annual Review*. 2005;11: 127–152. https://doi.org/10.1016/s1387-2656(05)11004-7

94. Seidler E. The tetrazolium-fomazan system: design and histochemistry. *Progress in Histochemistry*

and Cytochemistry. 1991;24(1): 1–79. https://doi.org/10.1016/s0079-6336(11)80060-4

95. Altman F. P. Tetrazolium salts and formazans. *Progress in Histochemistry and Cytochemistry*. 1976;9(3): 3–51. https://doi.org/10.1016/s0079-6336(76)80015-0

96. Rotilio G., Bray R. C., Fielden E. M. A pulse radiolysis study of superoxide dismutase. *Biochimica et Biophysica Acta (BBA) - Enzymology*. 1972;268(2): 605–609. https://doi.org/10.1016/0005-2744(72)90359-2

97. Fridovich I. Superoxide Radical and Superoxide Dismutases. *Annual Review of Biochemistry*. 1995;64(1): 97–112. https://doi.org/10.1146/annurev.bi.64.070195.000525

98. Fielden E. M., Roberts P. B., Bray R. C., Lowe D. J., Mautner G. N., Rotilio G., Calabrese L. The mechanism of action of superoxide dismutase from pulse radiolysis and electron paramagnetic resonance. Evidence that only half the active sites function in catalysis. *Biochemical Journal*. 1974;139(1): 49–60. https://doi.org/10.1042/bj1390049

99. Kalinina A. A., Belov D. V., Chelnokova M. V., Sokolova T. N., Moskvichev A. N., Razov E. N., Kartashov V. R. Electron acceptor compounds in the study of biocorrosion phenomena. *Korroziya: Materialy, Zashchita*. 2011;12:29–32. (In Russ.). Available at: https://elibrary.ru/item.asp?id=17241858

100. Sirota T. V. A Chain reaction of adrenaline autoxidation is a model of quinoid oxidation of catecholamines. *Biophysics*. 2020;65(4): 548–556. https://doi.org/10.1134/S0006350920040223

101. Misra H. P., Fridovich I. The univalent reduction of oxygen by reduced flavins and quinones. *Journal of Biological Chemistry*. 1972;247(1): 188–192. https://doi.org/10.1016/s0021-9258(19)45773-6

102. Misra H. P., Fridovich I. The role of superoxide anion in the autoxidation of epinephrine and a simple assay for superoxide dismutase. *Journal of Biological Chemistry*. 1972;247(10): 3170–3175. https://doi.org/10.1016/s0021-9258(19)45228-9

103. Bors W., Michel C., Saran M., Lengfelder E. Kinetic investigations of the autoxidation of adrenalin. *Zeitschrift Für Naturforschung C*. 1978;33(11-12): 891–896. https://doi.org/10.1515/znc-1978-11-1215

104. Burns J. M., Cooper W. J., Ferry J. L., King D. W., DiMento B. P., McNeill K., Miller C. J., Miller W. L., Peake B. M., Rusak S. A., Rose A. L. Waite T. D. Methods for reactive oxygen species (ROS) detection in aqueous environments. *Aquatic Sciences*. 2012;74(4): 683–734. https://doi.org/10.1007/s00027-012-0251-x

105. MacNevin W. M., Urone P. F. Separation of hydrogen peroxide from organic hydroperoxides. *Analytical Chemistry*. 1953;25(11): 1760–1761. https://doi.org/10.1021/ac60083a052

106. Pobiner H. Determination of hydroperoxides in hydrocarbon by conversion to hydrogen peroxide and measurement by titanium complexing. *Analytical Chemistry*. 1961;33(10): 1423–1426. https://doi.org/10.1021/ac60178a045

107. Bunker B. C., Nelson G. C., Zavadil K. R., Barbour J. C., Wall F. D., Sullivan J. P., Windisch C. F., Engelhardt M. H., Baer D. R. Hydration of passive oxide films on aluminum. *Journal of Physical Chemistry B*. 2002;106(18): 4705–4713. https://doi.org/10.1021/jp013246e

108. Belitskus D. Reaction of aluminum with sodium hydroxide solution as a source of hydrogen. *Journal of the Electrochemical Society*. 1970;117: 1097–1099. https://doi.org/10.1149/1.2407730

109. Heusler K. E., Allgaier W. Die kinetik der auflosung von aluminium in alkalischen losungen. *Werkstoffe und Korrosion*. 1971; 22(4): 297–302. https://doi.org/10.1002/maco.19710220405

110. Ribeiro T., Motta A., Marcus P., Gaigeot M.-P., Lopez X., Costa D. Formation of the OOH radical at steps of the boehmite surface and its inhibition by gallic acid: A theoretical study including DFT-based dynamics. *Journal of Inorganic Biochemistry*. 2013;128: 164–173. https://doi.org/10.1016/j.jinorgbio.2013.07.024

111. Ren T., Yang S., Jiang Y., Sun X., Zhang Y. Enhancing surface corrosion of zero-valent aluminum (ZVAl) and electron transfer process for the degradation of trichloroethylene with the presence of persulfate. *Chemical Engineering Journal*. 2018;348: 350–360. https://doi.org/10.1016/j.cej.2018.04.216

112. Meredith C., Hamilton T. P., Schaefer H. F. Oxywater (water oxide): new evidence for the existence of a structural isomer of hydrogen peroxide. *The Journal of Physical Chemistry*. 1992;96(23): 9250–9254. https://doi.org/10.1021/j100202a034

113. Jursic B. S. Density functional theory and *ab initio* study of oxywater isomerization into hydrogen peroxide. *Journal of Molecular Structure*: THEOCHEM. 1997;417(1-2): 81–88. https://doi.org/10.1016/s0166-1280(97)00059-6

114. Franz J., Francisco J. S., Peyerimhoff S. D. Production of singlet oxygen atoms by photodissociation of oxywater. *The Journal of Chemical Physics*. 2009;130(8): 084304. https://doi.org/10.1063/1.3080808

115. Chumakov A. A., Kotelnikov O. A., Slizhov Yu. G., Minakova T. S. Substantiation of the generation of oxywater zwitterions and singlet oxygen atoms from hydrogen peroxide molecules in aqueous solutions. *Bulletin of the South Ural State University. Series "Chemistry"*. 2018;10(4): 44–59. (In Russ., abstract in Eng.). https://doi.org/10.14529/chem180405

116. Shaitura N. S., Laricheva O. O., Larichev M. N. Study of the mechanism of low-temperature oxidation of microsized aluminum powder with water. *Chemical*

Physics. 2019;38(3): 9–23. (In Russ.). https://doi.org/10.1134/S0207401X19030087

117. Larichev M. N. Reaction of aluminum powders with liquid water and steam. In: (2014). *Metal Nanopowders*. Gromov A., Teipel U. (Eds.). Weinheim, Germany: Wiley-VCH Verlag GmbH & Co. KGaA. W.; 2014. p. 163. https://doi.org/10.1002/9783527680696.ch8

118. Larichev M. N., Laricheva O. O., Leipunsky I. O., Pshechenkov P. A. The reaction of aluminum particles with liquid water and water vapor is a promising source of hydrogen for the needs of hydrogen energy. *Proceedings of the Russian Academy of Sciences. Energy*. 2007;5: 125–139. (In Russ.). Available at: https://elibrary.ru/item.asp?id=9584641

119. Zang J., Klasky M., Letellier B.C. The aluminum chemistry and corrosion in alkaline solutions. *Journal of Nuclear Materials*. 2009;384(2): 175–189. https://doi.org/10.1016/j.jnucmat.2008.11.009

120. Deng Z.-Y., Ferreira J. M. F., Tanaka Y., Ye J. Physicochemical mechanism for the continuous reaction of γ-Al_2O_3-modified aluminum powder with water. *Journal of the American Ceramic Society*. 2007;90(5): 1521–1526. https://doi.org/10.1111/j.1551-2916.2007.01546.x

121. Rosliza R., Izman S. SEM-EDS characterization of natural products on corrosion inhibition of Al-Mg-Si alloy. *Protection of Metals and Physical Chemistry of Surfaces*. 2011;47: 395–401. https://doi.org/10.1134/S2070205111030129

122. Song W., Du J., Xu Y., Long B. A study of hydrogen permeation in aluminum alloy treated by various oxidation processes. *Journal of Nuclear Materials*. 1997; 246(2–3): 139–143. https://doi.org/10.1016/S0022-3115(97)00146-3

123. Ulanovskiy I. B. Hydrogen diffusion and porosity formation in aluminium. I. B. Ulanovskiy (Ed.). Moscow: Izdatelskiy Dom 'MISIS' Publ., 2015. p. 122.

124. Kaspzyk-Hordern B. Chemistry of alumina, reactions in aqueous solution and its application in water treatment. *Advances in Colloid and Interface Science*. 2004;110(1–2): 19–48. https://doi.org/10.1016/j.cis.2004.02.002

125. Belov D. V., Sokolova T. N., Smirnov V. F., Kuzina O. V., Kostyukova L. V., Kartashov V. R. Corrosion of aluminum and its alloys under the effect of microscopic fungi. *Protection of Metals and Physical Chemistry of Surfaces*. 2008;44: 737–742. https://doi.org/10.1134/S0033173208070151

126. Belov D. V., Belyaev S. N., Maksimov M. V., Gevorgyan G. A. On mechanism of biocorrosion of aluminum alloys D16T and AMg6 (Review). *Korroziya: Materialy, Zashchita*. 2021;10: 1–10. (In Russ.). https://doi.org/10.31044/1813-7016-2021-0-10-1-22

127. Lee S., Shin J. H., Choi M. Y. Watching the growth of aluminum hydroxide nanoparticles from aluminum nanoparticles synthesized by pulsed laser ablation in aqueous surfactant solution. *Journal of Nanoparticle Research*. 2013;15: 1473–1480. https://doi.org/10.1007/s11051-013-1473-0

128. Wefers K., Misra C., Bridenbaugh P. *Oxides and hydroxides of aluminum*. Alcoa Laboratories. 1987. 92 p.

129. Ahmed M., Qi Y., Zhang L., Yang Y., Abas A., Liang J., Cao B. Influence of Cu^{2+} ions on the corrosion resistance of AZ31 magnesium alloy with microarc oxidation. *Materials*. 2020;13(11): 2647. https://doi.org/10.3390/ma13112647

130. Sinyavsky V. S., Valkov V. D., Kalinin V. D. *Corrosion and protection of aluminum alloys*. Moscow: Metallurgiya Publ.; 1986. 386 p. (In Russ.)

131. Beaunier L. Corrosion of grain boundaries: initiation processes and testing. *Journal of Physique Colloques*. 1982;43(C6): 271–282. https://doi.org/10.1051/jphyscol:1982624

132. Krymsky S. V., Ilyasov R. R., Avtokratova E. V., Sitdikov O. Sh., Markushe M. V. Intergranular corrosion of cryorolled and aged aluminum alloy D16. *Protection of Metals and Physical Chemistry of Surfaces*. 2017;53: 1091–1099. https://doi.org/10.1134/S2070205117060144

133. Abramova M. G., Goncharov A. A. Intergranular corrosion of wrought aluminum alloys during full-scale and full-scale accelerated climatic tests. *Proceedings of VIAM*. 2019;11(83): 85–94. (In Russ., abstract in Eng.). https://doi.org/10.18577/2307-6046-2019-0-11-85-94

Author information

Denis V. Belov, Cand. Sci. (Chem.), Associate Professor, Senior Research Fellow, Federal Research Centre Institute of Applied Physics of the Russian Academy of Sciences (Nizhny Novgorod, Russian Federation).

https://orcid.org/0000-0001-7190-0477
belov.denbel2013@yandex.ru

Sergey N. Belyaev, Cand. Sci. (Chem.), Researcher, Federal Research Centre Institute of Applied Physics of the Russian Academy of Sciences (Nizhny Novgorod Russian Federation).

https://orcid.org/0000-0003-2346-9103
serg_belyaev@bk.ru

Received 29.12.2021; approved after reviewing 11.04.2022; accepted for publication 15.04.2022; published online 25.06.2022.

Translated by Valentina Mittova
Edited and proofread by Simon Cox